2012-12-14

Structural Design of Flexible ETFE Atrium Enclosures Using a Cable-Spring Support System

Ryan Paul Bessey
Brigham Young University - Provo

Structural Design of Flexible ETFE Atrium Enclosures

Using a Cable-Spring Support System

Ryan Paul Bessey

A thesis submitted to the faculty of
Brigham Young University
in partial fulfillment of the requirements for the degree of

Master of Science

Richard J. Balling, Chair
Paul W. Richards
David W. Jensen

Department of Civil and Environmental Engineering

Brigham Young University

December 2012

ABSTRACT

Structural Design of Flexible ETFE Atrium Roofs
Using a Cable-Spring Support System

Ryan Paul Bessey
Department of Civil and Environmental Engineering, BYU
Master of Science

This research designed and analyzed an innovative structural support system for ETFE (ethylene tetrafluoroethylene) atrium roofs between buildings. A cable-spring system was conceived, which is much lighter and more flexible than arches, frames, trusses, and beams which usually support ETFE roofs. Flexibility was a desirable property because the displacements may vary significantly among the buildings supporting the ETFE atrium roof during wind and seismic loading. The springs in the cable-spring system allow large differential displacements without exerting large support reactions on the buildings. The flexibility of the cable-spring system was compared to the cable-strut system which is used to support many other roofs. The concept of the cable-spring system was demonstrated by the design of an example problem and an experimental model. The example problem consisted of 20 m roof spans between buildings and differential displacements up to 8.5 cm. Conceptual design of the system consists of an array of intersecting cable-spring trusses that provide adequate drainage, venting, and repeatability. Detailed design includes the design of the ETFE cushion, truss depth, spring stiffness, cable sizes, and the telescoping tubes that enclose the springs. The ETFE cushions were analyzed with the MPanel software which is based on a computational process known as dynamic relaxation. The cable-spring trusses were analyzed using the principles of statics and large displacement geometry. Design curves and formulas were produced for spring sizes. A small scale experimental model was built to demonstrate the flexibility of the cable-spring support system. The weight of the atrium roof was estimated to be about 2.28 psf for the example problem. The analysis revealed that for the same spans and differential support movements the cable-spring support system had a 71% reduction in support reactions when compared to a cable-strut system.

Keywords: Ryan Paul Bessey, atrium, ETFE, cable-spring support system

ACKNOWLEDGMENTS

I wish to acknowledge my advisor Dr. Richard J. Balling for his guidance in the writing of this thesis. His ability to convey technical concepts, simply and concisely, will serve as a great example for me in my career. Going with Dr. Balling to China, for his Mega-structures class, was the highlight of my undergraduate experience and gave me inspiration to help me complete this work. I would also like to thank Timothy Akes, Andrew Askwith, and Barbara Derrick from the MPanel support team for temporarily granting me access to their unique analysis software while I am a student. The frequent correspondence with Andrew especially helped me with my analysis.

I would like to thank my wonderful wife for supporting me in my graduate studies and for tolerating my long hours away from home. She and my children make all my school work worth it. I would also like to thank all of my family members, many of which had a hand in sustaining me during my studies. My parents and my wife's parents in particular were very supportive emotionally, spiritually, and financially during this busy time of my life. Lastly I would like to thank the other students who worked with us on this project, especially Amy McCall for the data she supplied me on the optimized greenplex analysis.

TABLE OF CONTENTS

LIST OF TABLES

LIST OF FIGURES

1 INTRODUCTION

The major contribution of this work was to design and analyze a cable-spring support system for ETFE atrium roofs between buildings. Most conventional atrium designs use heavy glass, polycarbonate, or acrylic for the façade material. ETFE was used instead of these conventional materials primarily due to its light weight. ETFE also possesses many other desirable properties like high ductility, transparency, and insulation. ETFE is also self-cleaning, easily maintained, and requires minimal energy in production and recycling. Currently, most atrium roofs are supported by heavy and rigid frames, trusses, arches, or beams. These rigid support systems achieve flexibility by attaching the structures to rollers or rubber mounts at the supports. The cable-spring support system designed herein achieves flexibility within the structure instead of at the supports. Flexibility was pursued to reduce support reactions in case the supports experience differential displacements. The cable-spring support system can be compared to a cable-strut system which has also been used to support roofs. Cable-strut systems achieve significant weight savings but still have limited flexibility. Replacing the stiff compression struts with soft springs gives the cable-spring support system much more flexibility while maintaining the same weight advantages. Subsequent chapters in this thesis present a literature review on ETFE, roof support-systems, a conceptual design of an example problem, and a detailed design and analysis of the system.

The literature review on ETFE presents the many advantages of using ETFE in atrium roof applications. Research included material and chemical properties, ETFE cushion technology, weight, fire performance, insulation, transparency, maintenance, embodied energy and recycling, and decoration. Compiling this information also provides future researchers with a base knowledge of ETFE. Roof support systems including geodesic domes, cable tents, frames, arches, and cable-struts are also discussed to demonstrate the advantages and disadvantages of these systems. The literature review on these structures helps illustrate the differences between the cable-spring support system from other conventional systems.

This work presents the conceptual design of an atrium roof tailored to the needs of a specific example problem. A detailed problem statement of the design example is given to identify specific roof parameters like span and deflections. The support system was designed for spans over 20 m and deflections over 8.5 cm. Primary and secondary objectives for the atrium roof are also outlined. Among these are: prevent roof flutter; provide adequate slope and water drainage; provide capabilities for on-demand air ventilation; and to achieve a repeatable cable topology. The relative effectiveness of the proposed support system is demonstrated by also presenting the problems with other rejected design attempts.

A detailed design and analysis of certain components of the atrium roof is also presented. This includes an ETFE cushion, truss depth, spring stiffness, cables sizes, and the telescoping tubes that enclose the springs. To ensure that the final design was engineered with methods consistent with current ETFE design practices, software developed by tension membrane engineers was used. Among the many software packages used by tension membrane engineers are MPanel and MPanel FEA. MPanel was used to create the form of the ETFE envelope and MPanel FEA was used to analyze it using the computational techniques of dynamic relaxation.

Spreadsheets using statics equations and geometric nonlinearity were used to design the cables and springs. A small scale experimental model was also built to demonstrate the increased flexibility of the cable-spring system compared to a cable-strut system.

Conclusions on the conceptual design, the detailed design and analysis, and the experimental model are presented last. Key accomplishments and results on weight and flexibility are identified to illustrate the contributions of this work. Ideas for future research are also presented for consideration.

2 ETFE LITERATURE REVIEW

ETFE (ethylene tetrafluoroethylene) is a fluoropolymer developed in the 1940's by the American chemical company, DuPont. The original market for ETFE was anticipated to be petroleum, automotive, aerospace, and nuclear industries. Insulation material resistant to friction and abrasion and immune to other hostile environments such as radiation and extreme temperatures needed to be created for electrical wire insulation. During the development of ETFE, another innovative spin-off product called Teflon (PTFE) was invented (Vector Foiltec, 2012a). Architectural applications with ETFE began in the 1970's as a replacement for glass in greenhouse construction (LeCuyer 2008).

2.1 ETFE Cushions

While ETFE has been used as an insulating sheath for cable and electrical equipment it takes on a very different form in architectural settings. In such applications the ETFE is extruded into thin sheets referred to as foils that typically range from 50 μm to 300 μm in thickness. These can either be stretched into a single layer membrane or inflated into cushions using two or more layers that are heat welded and clamped around their perimeter. There are several different methods of creating the foil cushion which are shown in Figure 1 (Moritz and Hafner 2010).

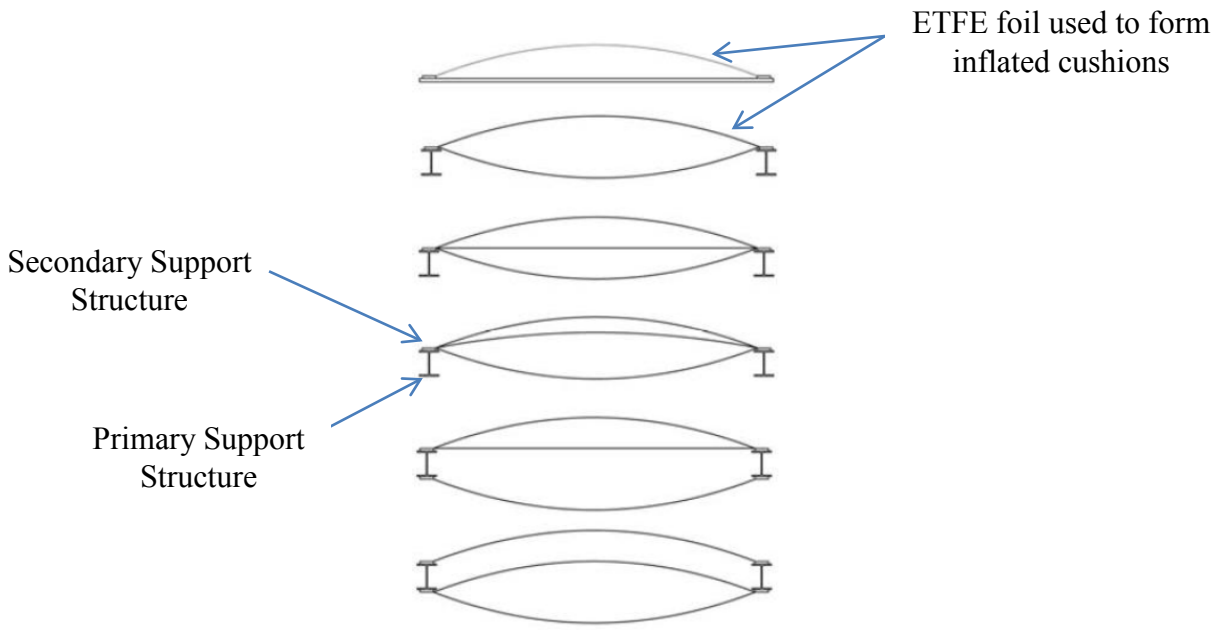

Figure 1: Common ETFE Foil Configurations

Primary structural systems typically support a secondary structure consisting of a gutter system and weather flashings. This secondary structure provides an attachment point for aluminum extruded flashings that clamp the ETFE cushion to the support frame (Figure 2) (LeCuyer 2008).

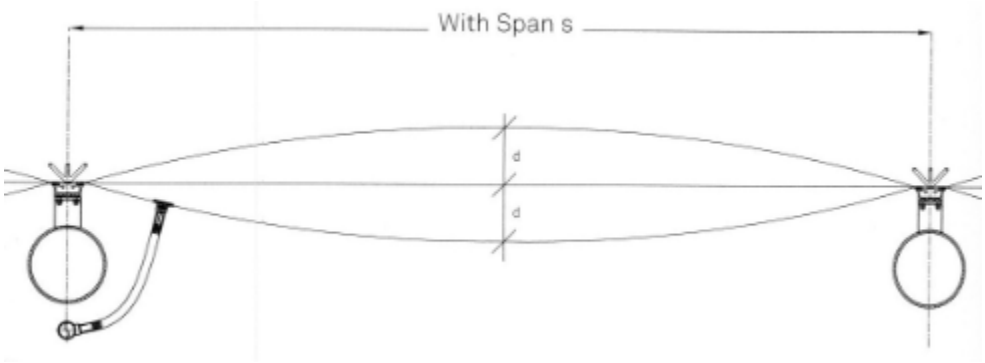

Figure 2: Connections of ETFE Cushions to Support Frame

Maximum glass panel spans are on the order of 2 m by 4 m, while ETFE can span much larger distances. Hexagonal cushions as large as 11 m across and 17 m rhombuses have been constructed for buildings in Europe. The larger ETFE cushion spans reduce the length of flashing at the edges of cushion. This improves the insulation value of the entire roof and

provides points of entry for water leakage and outside air. This reduction in supporting structure and flashing also contributes to the impressive weight savings attained by the light membrane itself. ETFE cushion's larger span results in a better climatic envelope for atrium applications than a traditional glazed roof.

Figure 3: Air Hose Connection to an ETFE Cushion.

The foil cushions can be inflated with an air hose and pump system similar to the one in Figure 3 (Buitink Technology 2012). Most ETFE cushion facades are inflated to a pressure between 200-600 Pa which is sufficient to resist most external loads such as wind or snow. Once the air hose is attached to the cushion it is inflated using a central air pump system that monitors the cushion's internal pressure, temperature, and humidity. Figure 4 shows a typical pump system for roof sizes around 1000 m^2 (Architen Landrell 2012a). Using cushion sensors the central air pump system also monitors external factors caused by weather such as wind pressures and directions, snow loading, temperature, humidity, and dew point. From the central pump and control system shown in Figure 5, the cushion's pressure can be adjusted to adapt to number of external stimuli (Architen Landrell 2012b).

Figure 4: Typical Inflation Unit.

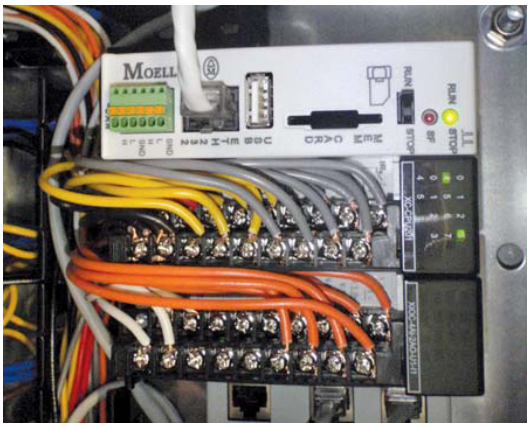

Figure 5: Cushion Pressure Control System

The pump system is meant to maintain pressure and not to produce airflow. A single inflation unit can pressurize about 1000 m^2 of ETFE cushions and consists of two backward air foil blowers powered by electric motors. One of the motors is rated at 220 Watts and is permanently on standby while the other, rated at 100 Watts, only operates about 50% of the time using half as much energy as a domestic light bulb (Cripps et al. 2001; Tanno 1997; Moritz and Hafner 2010; Barthel et al. 2003). In the event of system failure the cushions maintain their pressure for an additional 3-6 hours due to the use of non-return valves (Architen Landrell 2012a).

2.2 Chemical Properties

The primary ingredient in the manufacturing of ETFE is fluorite, a common mineral shown in Figure 6, which is combined with hydrogen sulphate and trichloromethane. These ingredients make chlorodifluoromethane, that by pyrolysis, yields tetrafluoroethylene (TFE). The tetrafluoroethylene monomer, shown in Figure 7, is mixed with the ethylene monomer, shown in Figure 8, to make the ETFE copolymer (LeCuyer 2008). The ethylene and tetrafluoroethylene monomers alternate forming n identical units that comprise the entire ETFE polymer as shown in Figure 9 (Polymers: a Properties Database 2012).

Figure 6: Sample of the Mineral Fluorspar.

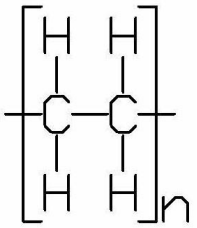

Figure 7: Structure of an Ethylene Monomer that Forms Polyethylene

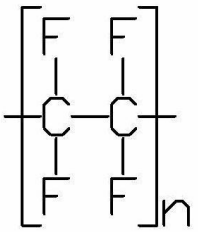

Figure 8: Polytetrafluoroethylene Molecular Structure

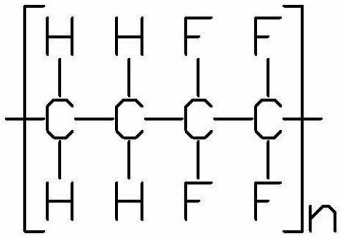

Figure 9: Polyethylene Tetrafluoroethylene

ETFE is a semi-crystalline polymer, meaning that it possesses both crystalline and amorphous phases. Amorphous qualities increase the flex life of a material, or the number of fatigue cycles until failure, while increased crystallinity decreases a material's resistance to fatigue. Semi-crystalline polymers have a degree of crystallinity between 30-70% with ETFE being about 33% crystalline (Moritz 2007). The crystalline regions of the microstructure, also called lamellae, are illustrated with the parallel bold lines in Figure 10 and Figure 11 while the amorphous regions are illustrated with the random curved lines (Winkler 2009).

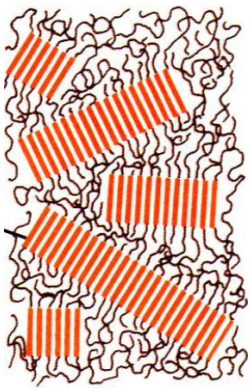

Figure 10: Semi-Crystalline Microstructure

Figure 11: Crystalline Structure Aligning with the Direction of Loading

Fluoropolymers are polymers that contain carbon, hydrogen, and fluorine. Polymers that only contain the carbon and fluorine are referred to as perflouropolymers, while those with the addition of hydrogen are called partially fluorinated polymers. ETFE is considered a partially fluorinated polymer. The addition of the hydrogen atom increases the hardness and toughness of the material but decreases its thermal stability. The introduction of the hydrogen also makes it less susceptible to creep (Ebnesajjad and Khaladkar 2005). Having a low degree of crystallinity and the addition of the hydrogen atom in the monomer of ethylene contributes to ETFE's unique material qualities that provide it with ample toughness and flexibility to be used as a pneumatic cushion. These chemical properties also contribute to its unique thermal characteristics but do not make it completely immune from creep which must be considered when designing cushions.

2.3 Mechanical Properties

While most construction materials are designed to maximize their strength and stiffness, ETFE's greatest structural asset is its ductility and flexibility. Being able to elongate between 250-650% allows the material to maintain its tension and stability despite large deflections. While the structural stiffness of many tall buildings is dictated by the prevention of cracking facades or breaking windows, ETFE absorbs all structural movements by constantly conforming to changing geometries. Inflated cushion systems, combined with ETFE's flexibility, also dampens the effects of sudden wind gusts on buildings reducing the required wind design loads for the structure. Figure 12 shows a stress-strain curve for a typical uniaxial test of ETFE (Moritz 2007). This graph is meant to illustrate qualitatively how ETFE strains under loads and does not represent an actual test specimen.

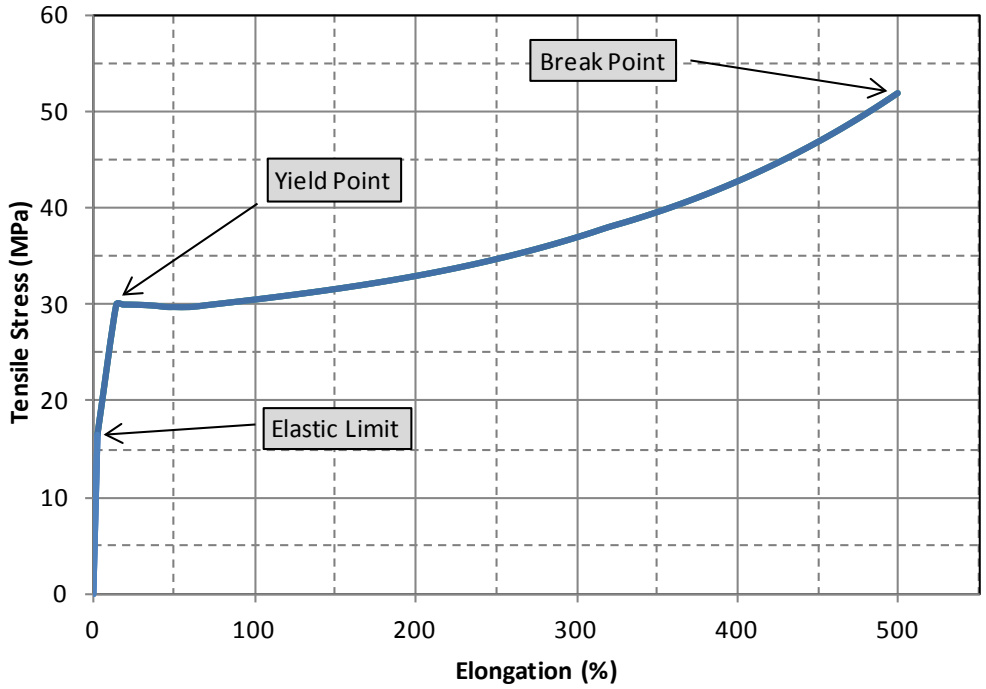

Figure 12: Generic Stress-Strain Curve for Uniaxial Tested ETFE Foil

One unique material quality that ETFE possesses is that it has a bilinear stress-strain curve followed by a large plastic region. The first change in stiffness is called the elastic limit and the second is the yield point. The elastic limit is the first point illustrated in Figure 12 where there is the first substantial change in stiffness. The yield point occurs when the material momentarily loses all of its stiffness and becomes highly nonlinear. After the yield point is surpassed the material goes into a stage of strain hardening in which it can elongate many times its own length, and almost double in strength. Typical mechanical properties for ETFE foils are displayed in Table 1 (Winser and Thompson 2003; Winser and Thompson 2002; Architen Landrell 2012b; Cripps et al. 2001; Robinson 2005; Galliot and Luchsinger 2011).

Table 1: ETFE Mechanical Properties

Mechanical Properties	Min	Max	Units
Modulus of Elasticity	300	1100	MPa
Poisson's Ratio	0.43	0.45	
Elastic Stress	15	18	MPa
Yield Stress	25	35	MPa
Ultimate Stress	40	64	MPa
Fracture Strain	250	650	%
Service Temperatures	-200	150	C
Melting Temperature	250	280	C
Hardness	31	33	MPa
Density	1.7	1.77	g/cm^3

The large range of mechanical properties for ETFE in Table 1 is due to variables including temperature, membrane thickness, and the local manufacturer. These ranges of mechanical properties make designing ETFE facades challenging and at times unconventional compared to typical construction practices.

2.4 Weight

Perhaps the most desirable property of ETFE foil systems is their light weight. With one foil layer weighing one percent of the weight of glass, the support structure for ETFE can weigh far less thus leading to longer spans. Even with the addition of the extra foil layers to produce an inflated cushion, aluminum extruded flashings, and an inflation tubing system, roof weights are often reported to be very light compared to glass roofs (Vector Foiltec 2012b).

2.5 Fire Performance

ETFE has the unique property of self-venting the products of combustion to the atmosphere. Under fire conditions any hot gases impinging on the cushions at a temperature above 200°C will cause the foil to soften and lose strength. As the foil is under tension from inflation, it fails and shrinks back from the plume, venting the fire to the atmosphere. Any fragments of the ETFE foil still present will be swept upwards by the plume. As the quantity of material used in the roof is so small and the ETFE is self-extinguishing, any drips of molten ETFE are non-burning and are prevented from falling to the ground. This self-venting and self-extinguishing feature of ETFE prevents the buildup of high temperatures under the roof and catastrophic structural collapse of the primary structure is prevented (Vector Foiltec 2012c).

2.6 Insulation

ETFE foil cushions perform very well as insulators. Originally developed as wire insulation for extreme temperature and chemical environments, ETFE surpasses the insulation value of glass in almost all building applications as shown in Table 2 (Robinson 2005). Insulation values are further increased with the introduction of the air pocket which acts similarly to double or triple pane glass. The cushions also have the ability to adjust their insulation value

by decreasing or increasing the pressure in the cushions, providing thermal adaptability once installed.

Table 2: Insulation Properties of ETFE and Glass

ETFE Cushion U Value		Glass U Value	
# of Foils	$W^{m-2}K$	$W^{m-2}K$	# of Panes
2	2.94	6.3	Single
3	1.96	3.2	Double
4	1.47	1.9	Triple
5	1.18		

2.7 Light Transmittance

ETFE foils are more transparent than glass in every wavelength of visible light, and have a significantly higher level of transparency in the ultraviolet light spectra (Figure 13). This is attractive for atria and especially for greenhouses since plants use the entire spectra of light for photosynthesis (LeCuyer 2008).

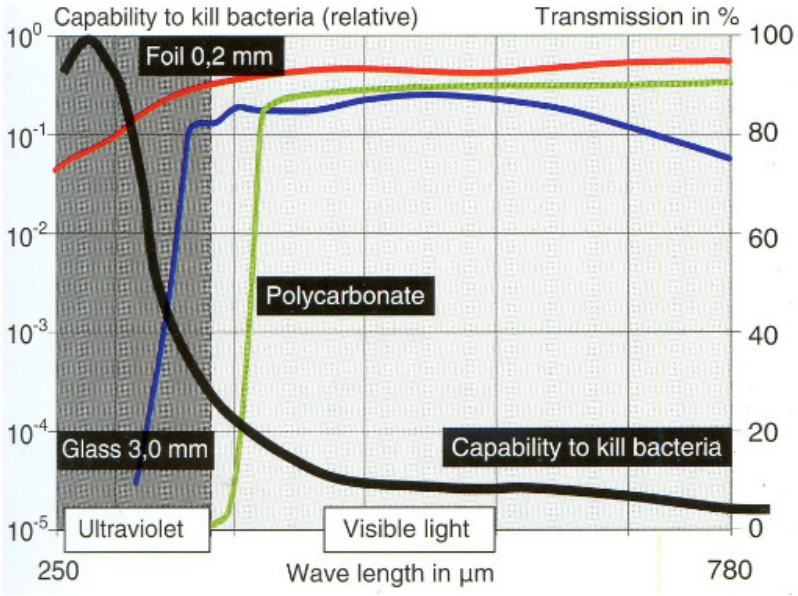

Figure 13: Light Transmittance of ETFE and Other Glazing Materials

ETFE foil at 200 µm wavelengths has higher transmittance than regular glass and polycarbonate within 250-780 µm wavelengths. Because ETFE lets through most UV light, it is resistant to UV degradation and discoloration, which is a common problem with other architectural glasses (Vector Foiltec 2012d).

While ETFE has high levels of light transmittance, this can have adverse effects on solar heat gain in buildings. Foils can be printed with an infinite variety of shading patterns that can block out light at varying amounts throughout the day. An example of foil printing is shown in Figure 14 (Koch 2004).

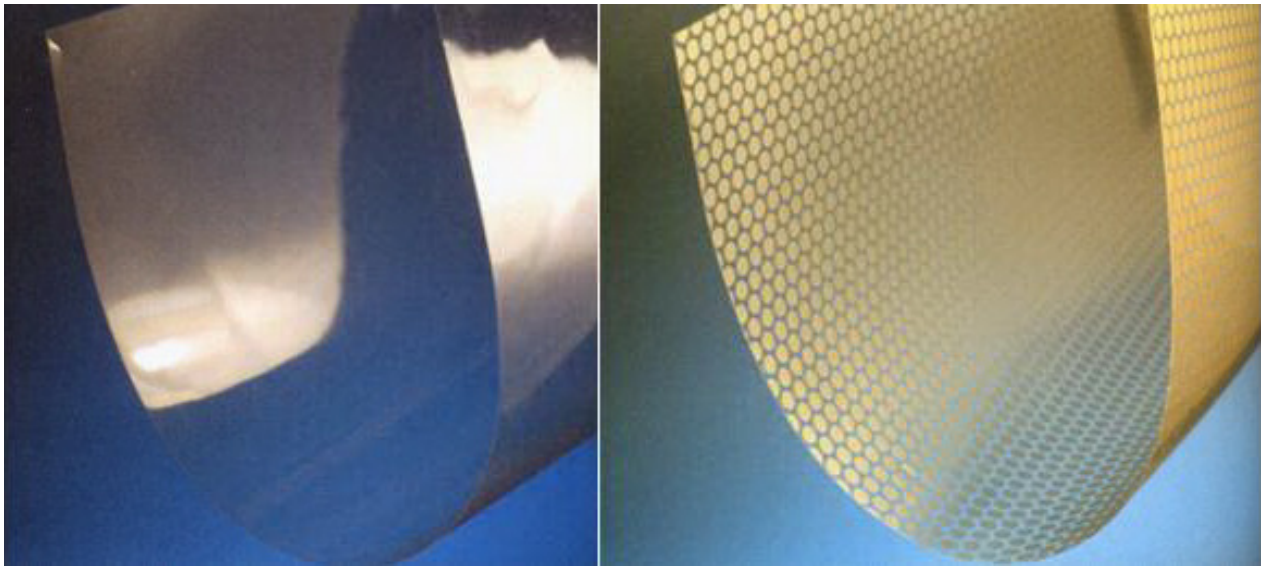

Figure 14: Clear ETFE Foil (left), Reflective Pattern Printed on ETFE Foil (right)

The outer and middle layer, within a three-layer system, can be printed with positive and negative patterns that let light through when the foils are separated and repel light when they are together. The position of the middle layer is controlled by the relative air pressures between the two chambers. As shown in Figure 15, when the pressure in the bottom chamber increases the foil layer inverts and presses up on the top layer thus blocking out light and controlling the building's solar heat gain (Vector Foiltec 2012e).

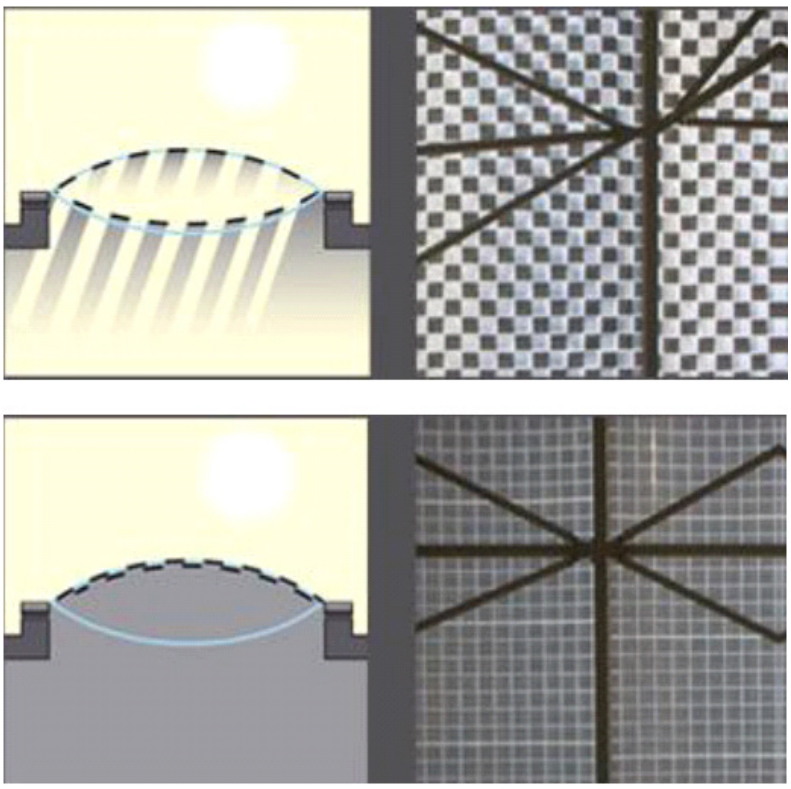

Figure 15: Section View of Variable Lighting 3 Layered Systems

ETFE's ability to dim or brighten the natural lighting in a building, with the simple adjustment of air pressure, has contributed to the choice of implementing this technology in many buildings today. Some of these buildings include Kingsdale School in London, shown in Figure 16 (Vector Foiltec 2012f), the Cyberbowl in Hanover, and the Art Center for the College of Design in Pasadena.

Figure 16: Kingsdale School, London

Recent research at MIT has proposed to combine three technologies into one intelligent building façade technology. Combining the use of ETFE cushions, with electrochromic windows, and pressure sensors would create a touch-responsive electrochromic ETFE cushion. This would allow for individuals to simply tap an ETFE cushion and have it change its transparent qualities just like any "smart window" today. Figure 17 shows the schematic of these three technologies being integrated into the same system (Cardoso et al. 2011).

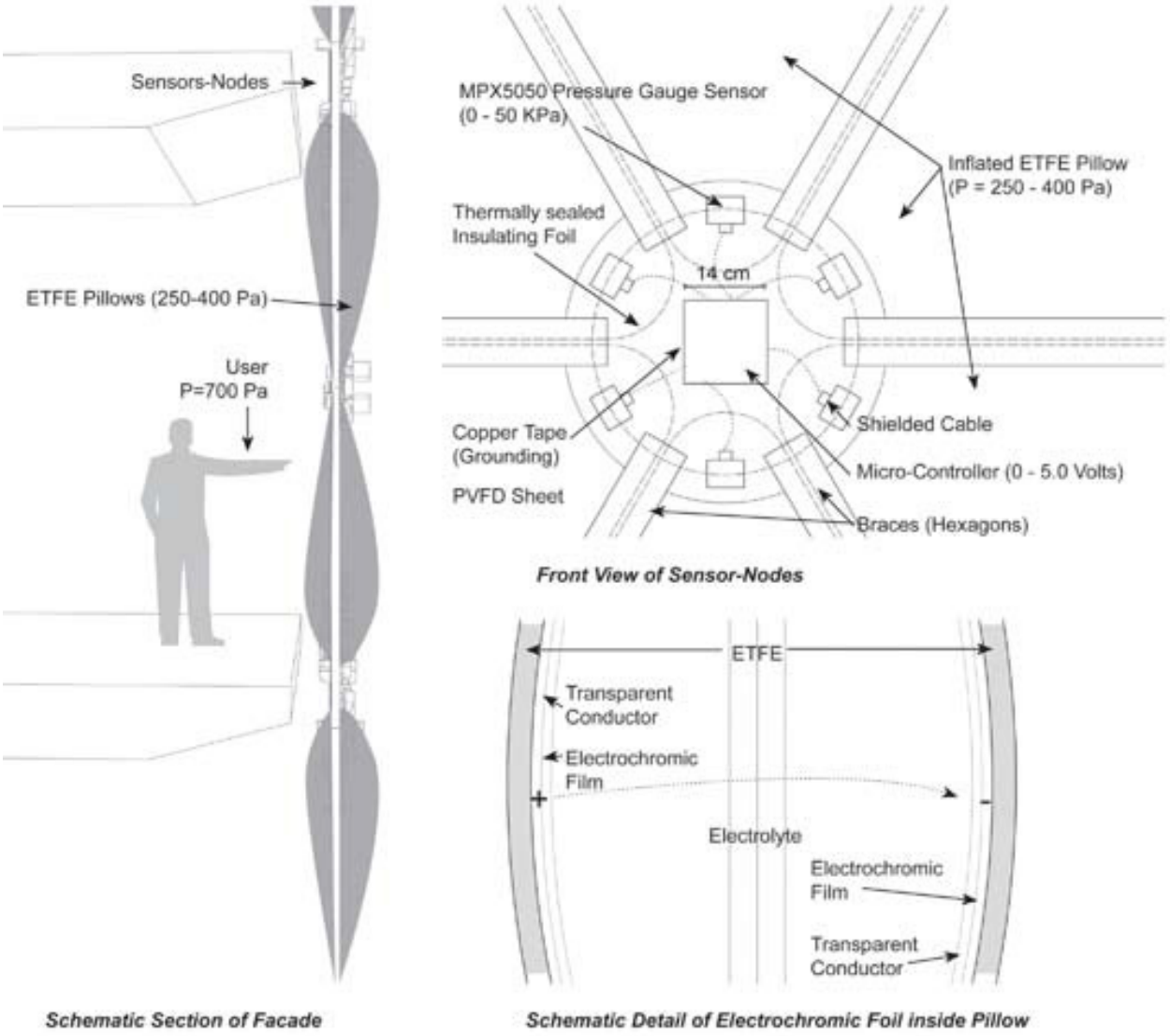

Figure 17: Schematic of Touch Responsive Electrochromatic ETFE Cushion Façade

Another recent technology that has adapted to the ETFE industry is the flexible photovoltaic strip. Continuous photovoltaic cells can be integrated straight into the upper foil of the ETFE cushion as shown in Figure 18, which protects the cells from weathering and is still transparent enough to let a high percentage of light through. Such systems contribute to the building's power supply reducing its energy demand on the city power grid (Solarnext 2012).

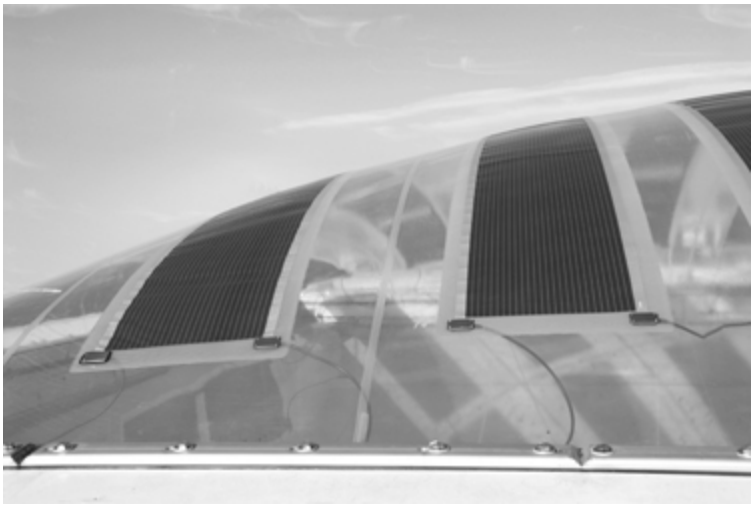

Figure 18: Photovoltaic Strips Integrated into ETFE Foils

2.8 Maintenance

Maintaining an ETFE roof has been reported to be less expensive than maintaining a glass roof due to the nonstick properties of ETFE (Winser and Thompson 2002). Similar to its chemical cousin, Teflon, ETFE is one of the smoothest substances known to man giving it self-cleaning properties that minimize the need for regular cleaning services. Dust or mineral deposits from snow or rainwater remain unattached to the ETFE and are immediately washed off during the next rain storm. Cleaning of the inside surface of the foil cushion may take place every 5-10 years but is rarely done due to the lack of necessity (LeCuyer 2008). According to a report provided by the Department of the Environment Transport and the Regions (DETR), Westminster Hospital calculated only £30,500 that would be spent on cleaning costs of their ETFE atrium for the 60 year lifespan of the building, as opposed to £104,700 for a glass atrium (Winser and Thompson 2003).

While the ETFE will not shatter like glass, it can be punctured by a knife or by birds. Tears or holes do not propagate or lengthen easily through ETFE foils due to its chemical properties. For tears less than 100 mm long, a patch of ETFE tape can be heat welded into place

preventing the need to replace entire panels like glass if cracks occur. In the case of full panel replacement, the ETFE is so light weight that it can be easily replaced without the need of scaffolding or lifting equipment. Servicing the roof with workers is not problematic either since the cushions can easily handle the weight of foot traffic (LeCuyer 2008).

2.9 Embodied Energy and Recycling

Embodied energy is the measure of required energy to produce a certain material including raw material extraction, manufacturing, and transportation. According to DETR the embodied energy for ETFE is an order of magnitude less than that of 6 mm glass due to the thinness of the material (Cripps et al. 2001). These values are reported in Table 3.

Table 3: Reported Embodied Energy of Glass and ETFE

Embodied Energy	ETFE Foil	6 mm Glass
(GJ/ton)	26.5	20
(MJ/m^2)	27	300

Recycling ETFE is also easy and energy efficient, making the process of reusing old cushions viable. The low melting point of ETFE makes the operation very inexpensive. Once melted down, the ETFE is extruded into the thin films used in cushion foil systems. While glass is recyclable, float glass used for architectural purposes is sensitive to impurities when recycled glass and virgin glass are combined.

2.10 Decoration

Another feature that greatly increases the value of ETFE foil cushions is the inclusion of LED's that can communicate written messages on the cushions or enhance the building's appearance. Many buildings (Figures 19-21) use such lights to increase the appeal of the

building. The customized lighting schemes can produce almost an unlimited variety of looks for the Allianz Arena, which greatly enhances the experience of spectators (Visit all the World 2012).

Figure 19: Photo of Allianz Arena in Germany

Other examples of variable lighting schemes are shown below in Figures 20 and 21

Figure 20: Heron Quays Light Rail Station

Figure 21: National Aquatics Center, Beijing

3 SUPPORT SYSTEMS

3.1 Free Standing Structures

3.1.1 Geodesic Domes – Eden Project, UK

Built in 2001, the Eden Project combined the aspirations of Buckminster Fuller with the technological advancements of ETFE films. The Eden project consists of eight interlinking geodesic domes as shown in Figure 22 (LeCuyer 2008).

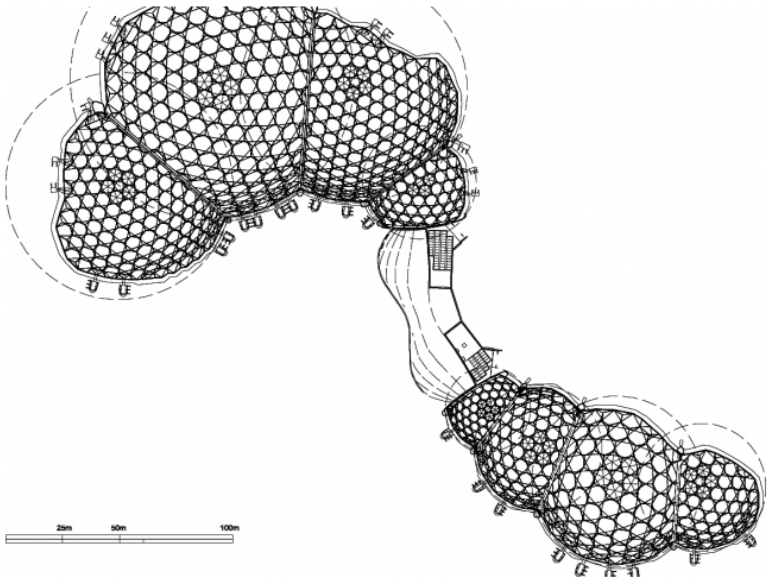

Figure 22: Plan View of Eden Project

The original design of the domes used only a single layer hexagonal pattern with 500 mm diameter circular hollow tubing. A much lighter option was presented by the project contractor who had developed a double layered hexagonal space truss. The outer layer consisted of ETFE cushions and 193 mm diameter circular hollow tubing with semi-fixed connections. The inner steel grid consisted of 114 mm diameter tube sections pin connected within a triangle and hexagon grid. Figure 23 shows the cushions, and the outer and inner steel grid. This system is referred to as a hex-tri-hex grid that provided considerable weight savings over a single layered grid.

Figure 23: Close Up of Double Layered Space Frame

Structural deflections of up to 20 cm were anticipated for the long span biomes. This is easily absorbed by the pliable ETFE membrane, thus making deflection and structural stiffness requirements far less demanding than if the façade was made from glass. ETFE's ability to

absorb energy from short term loads, like wind gusts, also allows the frames to be designed with lower wind speeds thus reducing the amount of required steel even more. The combination of ETFE's material advantages and the efficient space frame design for the Eden biomes resulted in a structure that actually weighs a little more than the air it encloses (667 tons of steelwork vs. 536 tons of air) (Vector Foiltec 2012g). This is truly an accomplishment that Buckminster Fuller would envy.

While considerable weight was saved, by using two hexagonal steel grids as opposed to one, the number of expensive nodes, and the fabrication complexity dramatically increased. This motivated the designers to greatly increase the size of the ETFE panels to reduce the number of nodes that had to be fabricated. Cushion sizes range from 5 to 11 meters across, which is substantially larger than any other previous ETFE project. One of these cushions is shown in Figure 24 (LeCuyer 2008).

Figure 24: Installation of ETFE Cushion

Wind loads on the structure were to be determined using scaled models due to the unconventional geometry and site topography. The study indicated that the surroundings of the building provided sufficient shelter against aggressive wind loads. Since the 50 m structure was constructed at the bottom of a large pit with 60m walls, the structure was classified as a below ground structure (Jones and Guthrie 2003).

Figure 25: Picture of Four Biomes Constructed for Eden Project

Other structural loads included differential settlement of the foundations, drifting snow between cushions and biomes, uniform snow loads, ponding of water, and temperature loads between the extremes of -10° and 50° C. Due to the domed shape of the structure the steel was granted space to 'breath' in case of differential temperature loading. In the case of power failure and subsequent deflation of the ETFE cushions, each biome is designed to be able to hold up the weight of 6 flooded cushion panels at the tops of the biomes (Jones and Guthrie 2003). Localized snow drifts between the biomes were also designed for by building intersecting trusses that arch between the individual domes. While the trusses could support the weight of drifting snow between biomes, the ETFE cushions along these arches had to be supported on the underside with a thin stainless steel cable net. These trusses and cable nets are illustrated in Figure 26 (LeCuyer 2008).

Figure 26: Arched Trusses and Cable Nets.

Figure 27: Double Layered Hexagonal Grid

3.1.2 Tents - Khan Shatyr Entertainment Center, Kazakhstan

The Khan Shatyr Entertainment Center is the world's largest tent and is built in the nomadic land of Kazakhstan where tent building has been mastered through the centuries. The architectural design was completed by Norman Foster and Partners while Buro Happold was responsible for the structural design. The 100,000 m^3 building was to appear elegant and spacious while also being able to withstand extreme loads and temperature differentials. Snow loads of up to 7 metric tons per square meter governed the overall shape of the structure. Creating a high peak with steep sides, as shown in Figure 28, eliminated the problem of ponding under snow and rain water, a design feature that must be used with roof structures that undergo large out-of-plane deformations (Vector Foiltec 2012h).

Figure 28: Exterior of the Khan Shatyr Entertainment

The vertical cables are designed to resist positive wind pressures while the horizontal hoops resist wind suction (LeCuyer 2008). The vertical cables also act as gutters to drain water off the structure, and the horizontal hoops were all tilted to prevent water from being trapped.

Cables were sized to be 32 mm in diameter and were attached to the ETFE cushions with aluminum extrusions as shown in Figure 29 (Winser and Thompson 2003).

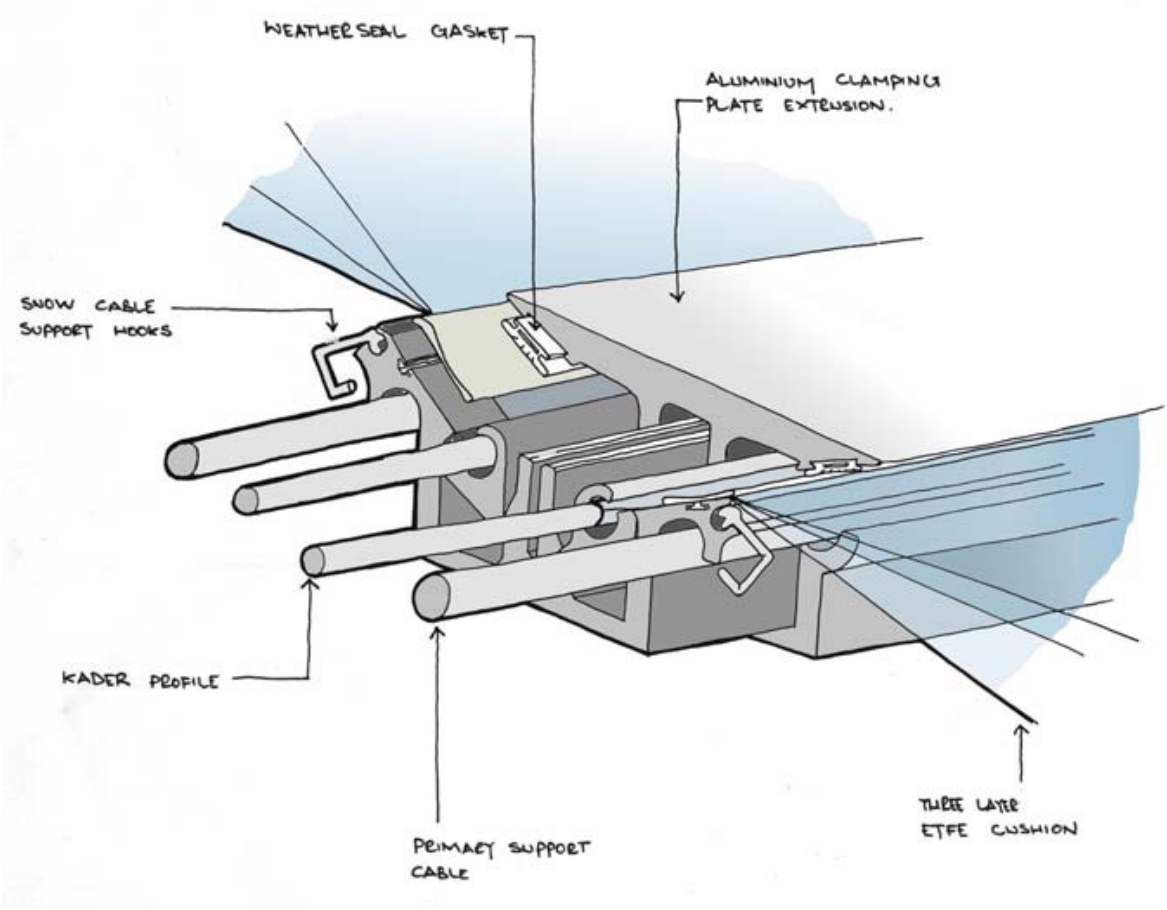

Figure 29: Attachment Method of ETFE Cushions to Cables.

This water tight and insulated connection allows for ETFE to attach to a variety of cable sizes and gives attachment points for stainless steel wire net reinforcing on the underside of the cushion to resist heavy snow loads. The many circumferential hoops circling the tent had to allow for expansion and contraction as the entire tent would deflect up to a meter at the top. A rigid ring had to be avoided, so an alternating circumferential cushion joint was designed in its place to allow for these deformations to occur without high stress concentrations. The combination of cables and flexible connections allowed for the steel structure to exhibit flexible qualities like the ETFE it supports (LeCuyer 2008).

Figure 30: Interior of the Entertainment Center

The radial cables are prestressed unusually high for a tent structure (as much as 80% of the peak load). The cables attach to the masts by means of a basketlike hub of steel props that feature a 20 m diameter ring. Between the tops of the tripod legs and the steel hub sit several bearings that allow the hub to move with the cable net to dissipate high wind induced stresses at the connection.

The massive support structure was designed to be a tilted tripod that forms a stable mast for the whole tent as shown in Figures 31 and 32 (Vector Foiltec 2012h). The back tripod leg is a vertical truss column with a length of 60 m and the two front legs are tilted 30 degrees from vertical and are both 70 m long. The compression members within the columns are comprised of 1 m outer diameter tube steel. The back leg was constructed using 60 mm thick steel while the front two legs used 25 mm thick tube steel. The legs widen their moment of inertia at the midpoints to resist the forces that would make them buckle (Reid 2009).

Figure 31: The Three Tripod Legs

Figure 32: Attachment Points of the Tripod Legs.

Figure 32 shows that the legs connect to the base building via 0.5 m diameter pins that are connected to reinforced concrete plinths approximately 4 m in diameter. The plinths are inclined to match the angle of the front legs and allow each of the legs to rock slightly in order to not pass on any bending moments into the concrete. Concrete piles up to 30 m in depth were used, under the plinths, to ultimately resist the high point loads of 30,000 kN and 80,000 kN produced by the front and back tripod legs (Reid 2009).

3.1.3 Cable-Strut Systems –Truck Depot, Germany

The truck depot for the Office of Waste Management in Munich, Germany is one example of a cable-strut roof system. While this system is not supporting ETFE cushions the PTFE coated glass fiber membrane performs in a similar way. This roof structure spans a total area of 8,400 m^2 which provides a safe covering for refuse collection vehicles (Koch 2004).

Figure 33: Exterior of Truck Depot

Figure 34 shows that the underside of the roof is supported by free standing columns that sit on the reinforced concrete parking deck. Due to asymmetric wind loading the column footings needed to be flexible to allow for base rotations. Between each of the columns is a cable-strut system that spans the gap between supports. The cable-strut system is comprised of two intersecting sets of cables forming top and bottom chords and a strut. The strut separates the cables forcing them into tension and the strut into compression.

Figure 34: Cable-Strut System Supporting the Membrane between Columns

Notice that the gravity loads are carried by the bottom cables while the top cables and membrane resist wind suction. Under uniform loading the columns only resist vertical loads since all cable forces are laterally resolved by other cables. At the edges of the free standing

structure the lateral loads are unbalanced and need to be resisted by an exterior structure. This structure is a set columns and guy cables that wrap the perimeter of the entire roof as can be seen in the lower left corner of Figure 33. Figure 35 shows that the cable strut system consists of a tensioned cable and membrane peak and a tension cable valley. This geometry gives the normally unstable membrane and cables the proper stability and stiffness to resist loads.

Figure 35: Cross Section of Cable-Strut System

The bottom cables of the cable-strut system are 22 mm in diameter and are attached to the struts and columns using fork elements as illustrated in Figure 36 (Koch 2004).

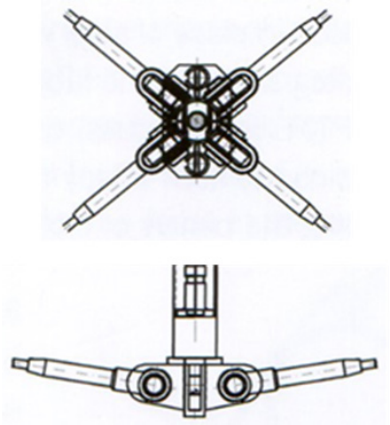

Figure 36: Fork Element Used to Attach the Cables to the Struts

A 21 mm diameter cable was welded into the PTFE membrane for reinforcing the upper umbrella surface. The entire structure is prestressed with the strut shown in Figure 37.

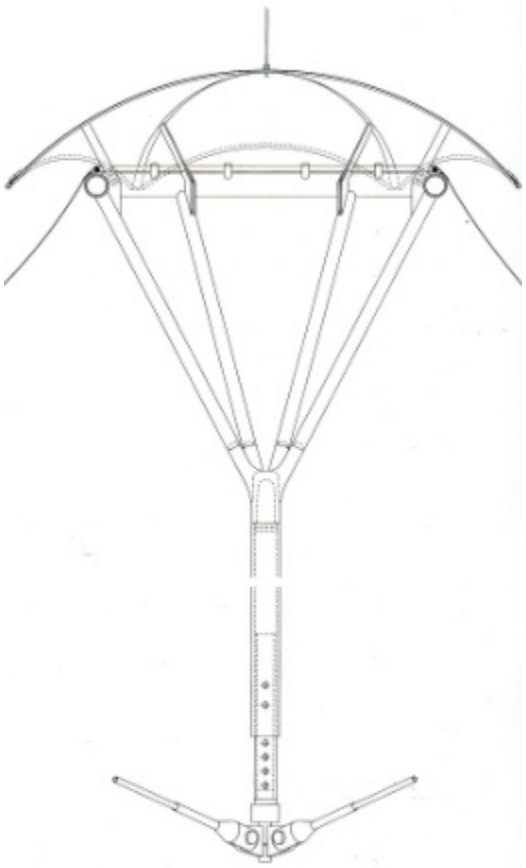

Figure 37: View of Strut with Bottom Jack

The compression struts can be prestressed by hand with the use of jacks mounted to the bottom. The jack has an adjustable length of 1 ft which applies load to the steel ring at the apex of the umbrella. This presses up and out on the PTFE coated glass fabric. The 1 mm thick membrane has a tensile strength of 130 kN/m (Koch 2004). The strength efficient cables and thin membrane façade result in an extremely light weight roof covering. However the stiff compression struts resist any lateral separation between the support columns, causing high reactions at the cable and column joints.

3.2 Building-Supported Structures

3.2.1 Frameworks - Parkview Green Plaza, China

Consisting of four high rise buildings, surrounded by glass walls and an ETFE roof, Parkview Green seeks to create a business park completely sheltered from the elements. ETFE foil cushions were used to span over the tops of the skyscrapers forming a slanted roof. Figure 38 shows an exterior view of this slanted ETFE roof (Vector Foiltec 2012i). ETFE's weight significantly reduced gravity and lateral loads on the four buildings.

Figure 38: Exterior of Parkview Green

This reduction of load on the buildings also had benefits in the natural lighting of the atria between buildings. Less structural material allows more light to enter the interior. While still reaping the benefits of being sheltered from the environment, the ETFE membrane allows the public atria space to be classified as open space for fire purposes. Venting of heat and smoke

through the ETFE membrane prevents the rapid spread of fire from building to building and helps the building pass stringent local fire codes. As the roof spans over the buildings it is attached to the roof with simple ball and socket joints to transfer only vertical loads to the four skyscrapers. A close up picture of this joint is shown in Figure 39.

Figure 39: Close Up of Ball and Socket Joint

As shown Figure 40 the main structural system consists of a two dimensional frame of beams. Above this sits the secondary structure to which the ETFE cushions are attached. Each of the ETFE cushions used 2 or more layers of foil at 100 to 250 microns thick. Cushions were cambered at 15-20 percent of their span and had an inflation pressure of 250 Pa (Figure 40).

Figure 40: Close up of ETFE Cushions

Figure 41: Interior of Parkview Green

Parkview Green illustrates ETFE's potential for atria construction in urban settings, and demonstrates many positive contributions to a city's ecological goals. Due to the contributions of ETFE and many other green building features, the building system has achieved a LEED Platinum Certification and has been named the best green building in Asia (Vector Foiltec 2012i).

3.2.2 Arched Roof – Forsyth Barr Stadium, New Zealand

The arched roof of the Forsyth Barr Stadium in Dunedin, New Zealand is the world's only permanently covered stadium to boast a natural turf. This was made possible due to the high transparency of ETFE in all wave lengths used for photosynthesis. A total of 20,500 m^2 of transparent ETFE covered the field area (Vector Foiltec 2012j).

Figure 42: Interior of Forsyth Barr Stadium

Supporting the nearly 300 double layered cushions are 5 external arch trusses that span 105 m from the tops of stadium seats. With an internal clearance of 37 m and a maximum height of 47 m, the 10 m tall external arch trusses were all that the stadium needed to hold up the light weight ETFE cushions. Between each of the arches is a series of flat trusses that support four long inflated ETFE cushions. Each flat truss spans 20 m between each arch truss segment. Internal and external views of the support structure are clearly seen in Figures 42 and 43.

Figure 43: Exterior of Forsyth Barr Stadium

While elegant and spacious, the intricate truss work for the roof and its side supports required a staggering 20,642 members weighing as much as 3,887 tons. Many of these members were trial fitted in the factory in massive jigs to assure that they would fit during the erection of the structure on site (SCNZ 2011).

Figure 44: Close Up of Trusses and Connections

The two bottom chords of the arch trusses sat 10 meters apart while the single top chord was elevated by 10 meters at its midspan. The 200 ton arch trusses used 71,000 bolts in assembling the 20,642 members fit with flange connections on their ends. This required very meticulous planning on the part of the fabricators (SCNZ 2011).

Figure 45: Fabrication Process

A predetermined bolting sequence was also produced by the engineers so that no bolt failures occurred during the erection process. All bolts were tightened to a third of their required torque first, and then using a hydraulic wrench, the riggers tightened the bolts to two thirds of the required torque. In phase three, all bolts were tightened to their full torque and then released to ensure that there were no bolt failures anywhere in the structure. Once all bolts were verified to be intact, the whole structure was reassembled together again to their full torque in the same bolting sequence as before (SCNZ 2011).

As the largest enclosed stadium in the southern hemisphere and as the venue to a number of prestigious sporting and cultural events, the Forsyth Barr Stadium has made and will continue to make an impact on the world. It is not only an outstanding demonstration of engineering but a testament to the benefits of light weight ETFE in the design of wide-span roof structures.

4 CONCEPTUAL DESIGN EXAMPLE

4.1 Problem Statement

The design example in this thesis consists of the design of Atria for an urban form called a greenplex. As shown in Figure 46, a greenplex combines tall buildings, sky bridges, and ETFE atria located between the buildings.

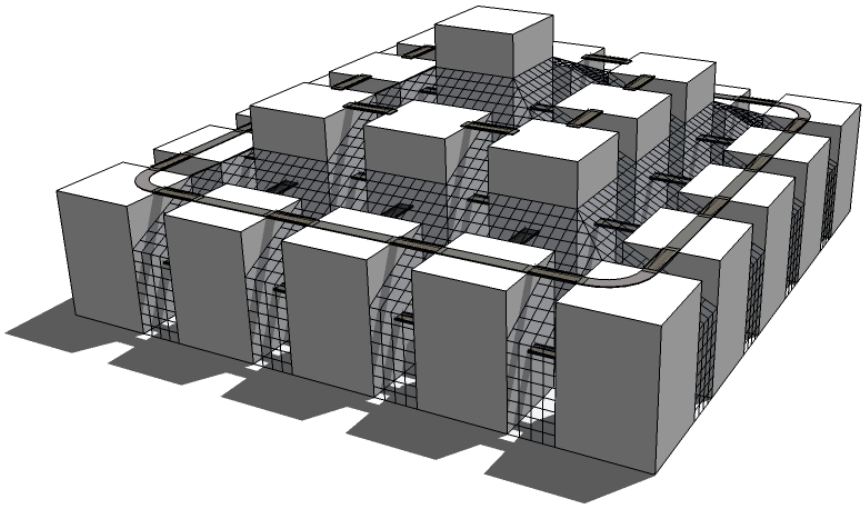

Figure 46: Greenplex of 25 Buildings

The greenplex is a new urban form that possesses major advantages over exposed disconnected skyscrapers. First, occupants are sheltered from severe weather. Second, the greenplex is a car-free zone which means less air pollution, noise, street congestion, traffic accidents, wasted time, expense, and obesity. Third, the greenplex is 3D walkable network that reduces travel time and provides multiple escape routes in emergency situations. Fourth, the

exposed surface area is far less than that of exposed skyscrapers which dramatically reduces energy consumption for heating and air conditioning. The ETFE atria were designed for the 25 building greenplex shown in Figure 46. **The same process can be used to design ETFE atria between any set of buildings.**

There are two primary objectives in the design of the ETFE and its support system. **The first primary objective is that it must be light weight,** in order to minimize the vertical load on the buildings. For this reason, a cable support system was used, which is inherently lighter than arch or frame systems. **The second primary objective is that the ETFE support system must be flexible** enough to accommodate large differential displacement between the buildings due to wind and seismic loading. Furthermore, the horizontal forces exerted by the system on the buildings must be minimal. Clearly, cable-strut systems, frames, arches, truss, and beams do not possess such flexibility. The major contribution of this thesis is the development of a new and innovative ETFE support systems utilizing springs and cables that possesses tremendous flexibility while exerting minimal horizontal forces on the buildings.

Secondary design objectives for the system include: 1) provide adequate support to prevent flutter in the ETFE cushions and support system; 2) provide adequate slope to control water drainage; 3) provide capabilities for on-demand air ventilation; 4) design a repeatable topology that makes possible the incremental construction of greenplex buildings overtime.

4.2 Conceptual Design

The conceptual design of the ETFE support system for the 25 building greenplex example is shown in Figure 47.

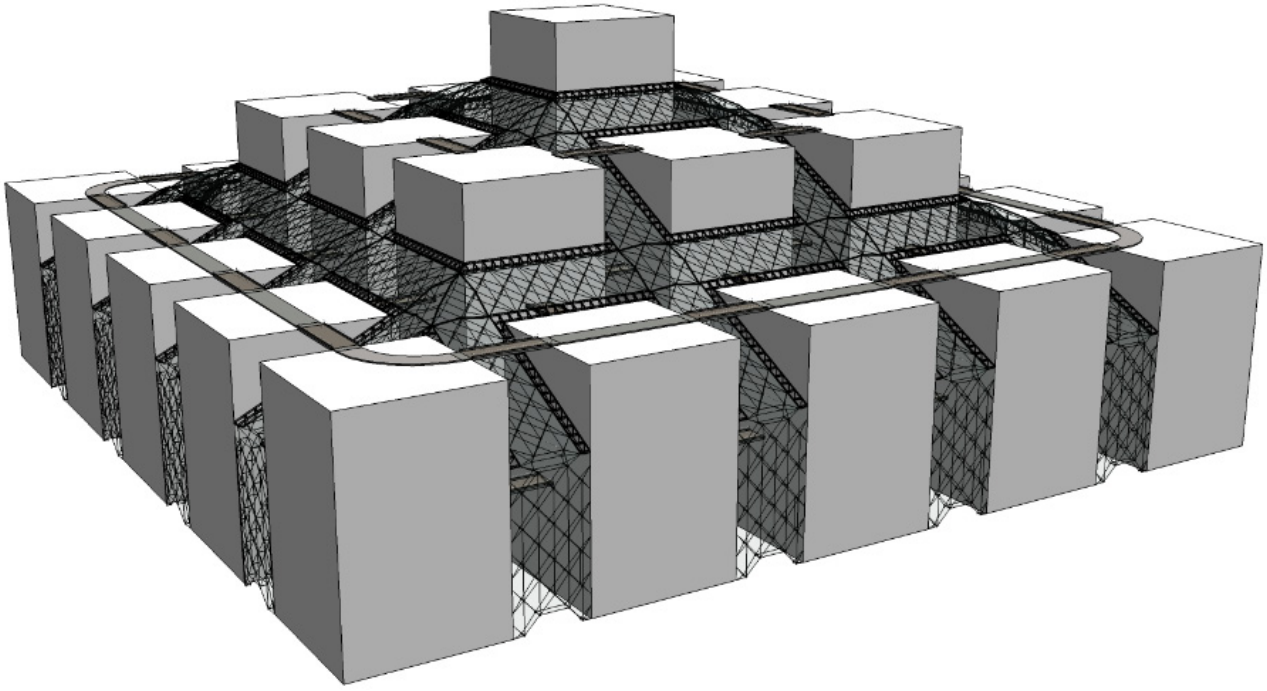

Figure 47: View of Entire Greenplex

Note the repeatability in the form. Controllable air vents are located at the ETFE building interfaces as shown in Figure 48.

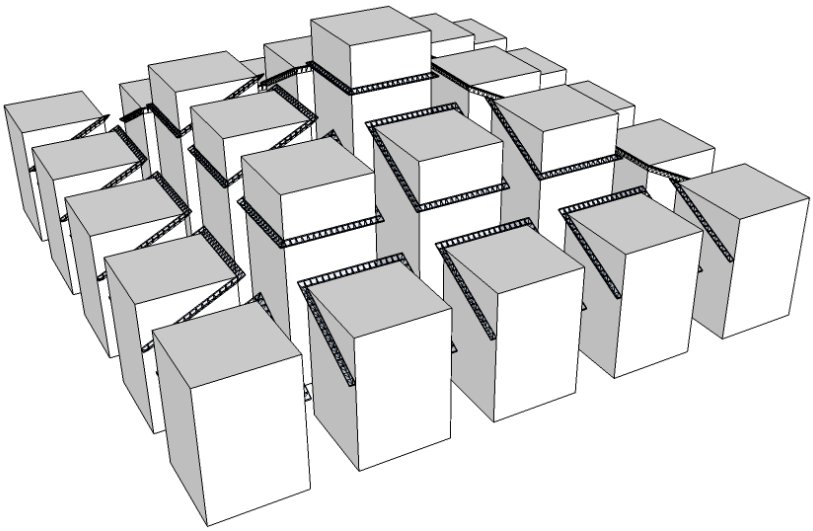

Figure 48: Air Vents that Wrap the Perimeter of the Buildings

The fundamental repeatable element in the greenplex support system is the cable-spring truss shown in Figure 49. Note the ETFE cushions are attached to the top cable.

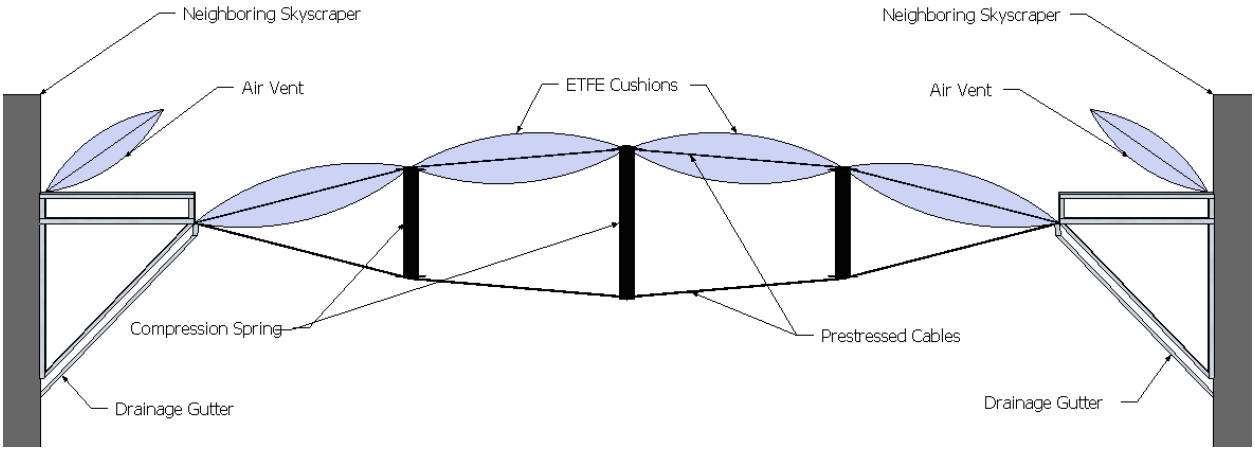

Figure 49: Cross Section of Cable-Spring Truss

These trusses span between the buildings in both diagonal directions as shown in Figure 50. Note that the trusses intersect each other at right angles.

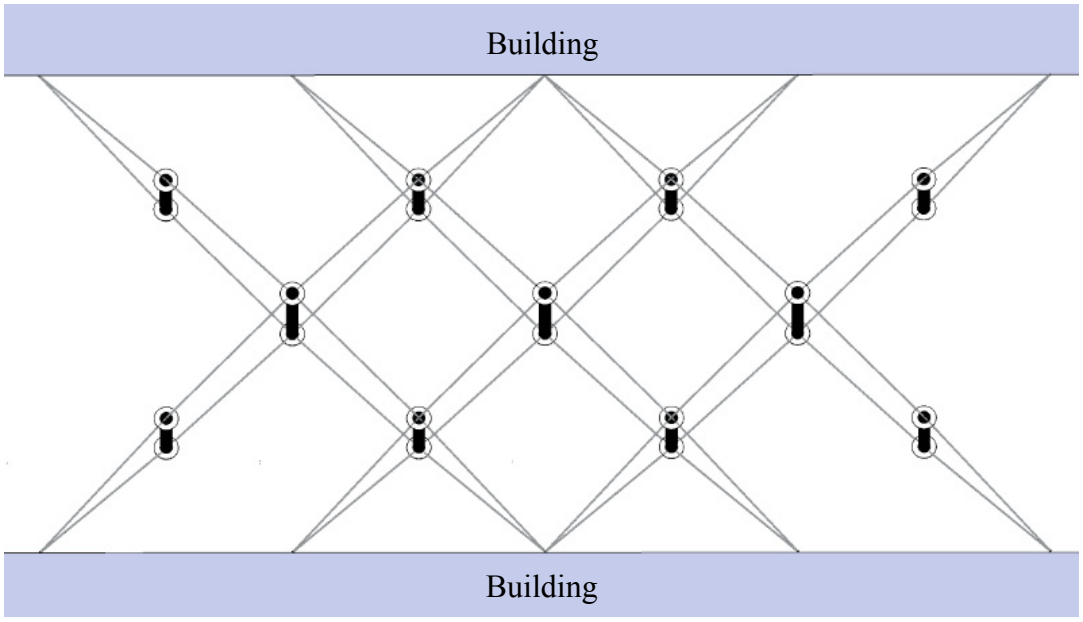

Figure 50: Repeated Cable-Spring Trusses

The vertical springs are enclosed inside a telescoping steel tube consisting of two cylindrical pieces one inside the other as shown in Figures 51 and 56. Note that each cylindrical piece has an end-cap to which the cables of the two intersecting trusses are attached.

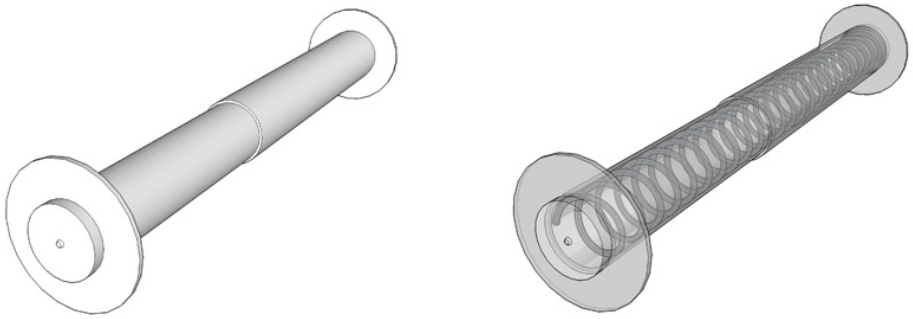

Figure 51: Isometric View of the Spring and Telescoping Tubes

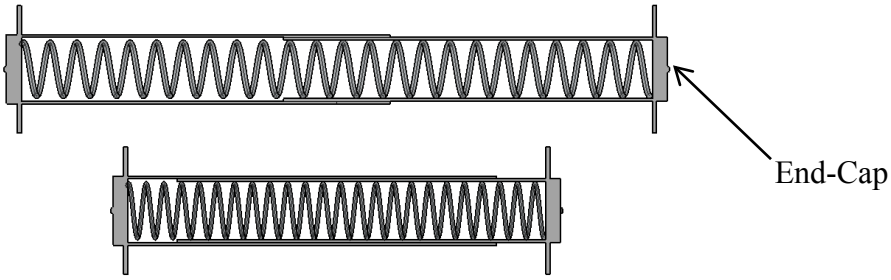

Figure 52: Expanded and Contracted Springs

As the roof supports displace away from each other, the springs compress and the cable-spring truss lengthens as shown in Figure 53.

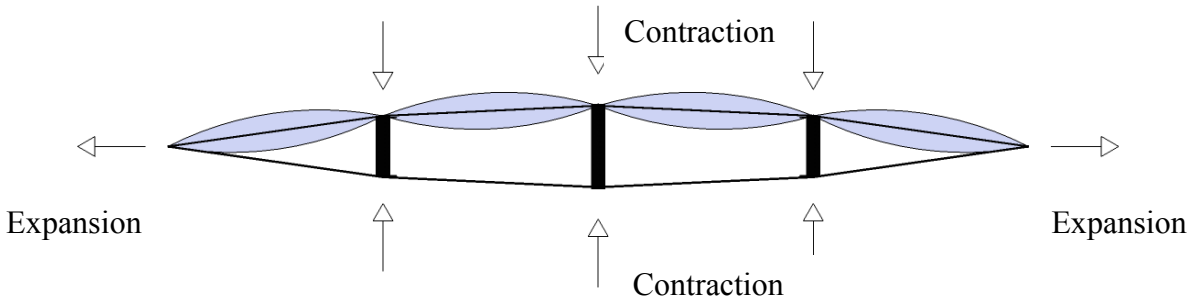

Figure 53: Expansion of Cable-Spring Truss Under Building Separation

The horizontal force exerted on the buildings is far less than with any system consisting of cables without springs. The system is prestressed so that the **springs remain in compression and the cables remain in tension under all loading conditions.** This insures that the cable-spring truss holds its shape as shown in Figure 54 and flutter is prevented.

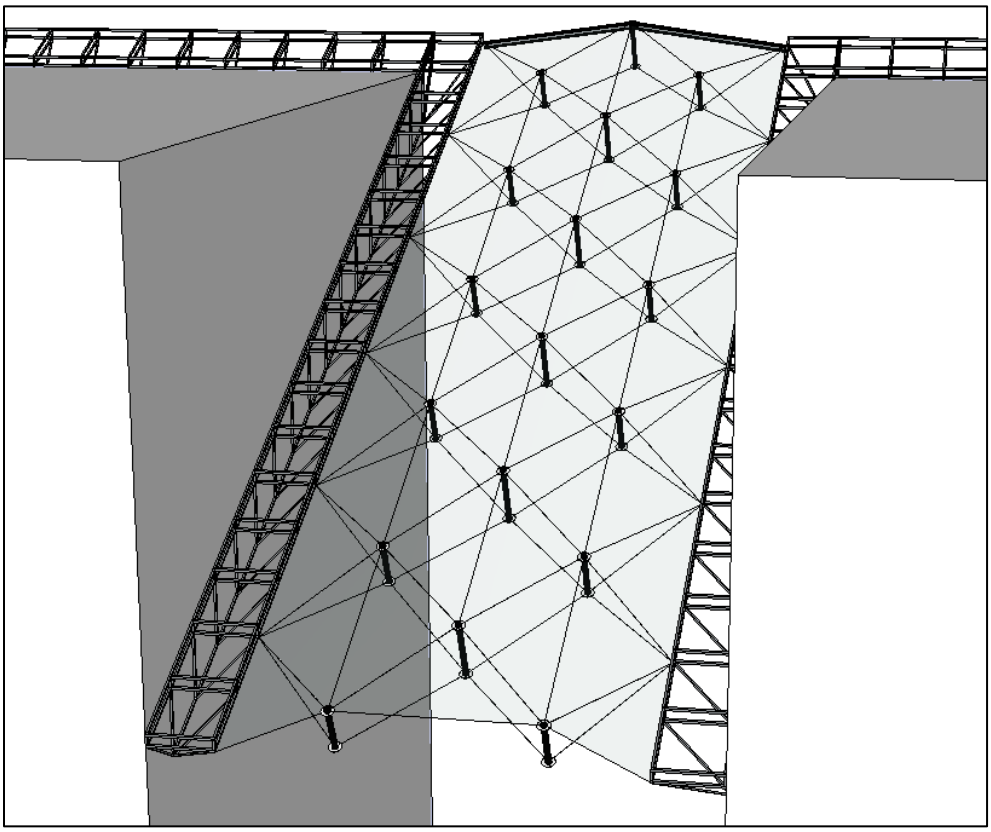

Figure 54: Shape of the Cable-Spring Truss Held by Buildings

Additional cables parallel to building edges are added to divide quadrilateral cushions into triangular cushions as shown in Figure 54, in order to decrease cushion deformation. Since these cables are parallel to building edges, they do not expand and contract as the buildings displace.

The depth of the springs also insures that rainwater drains to the building interfaces, as shown in Figure 55, where it is collected in gutters below the air vents (Figure 49).

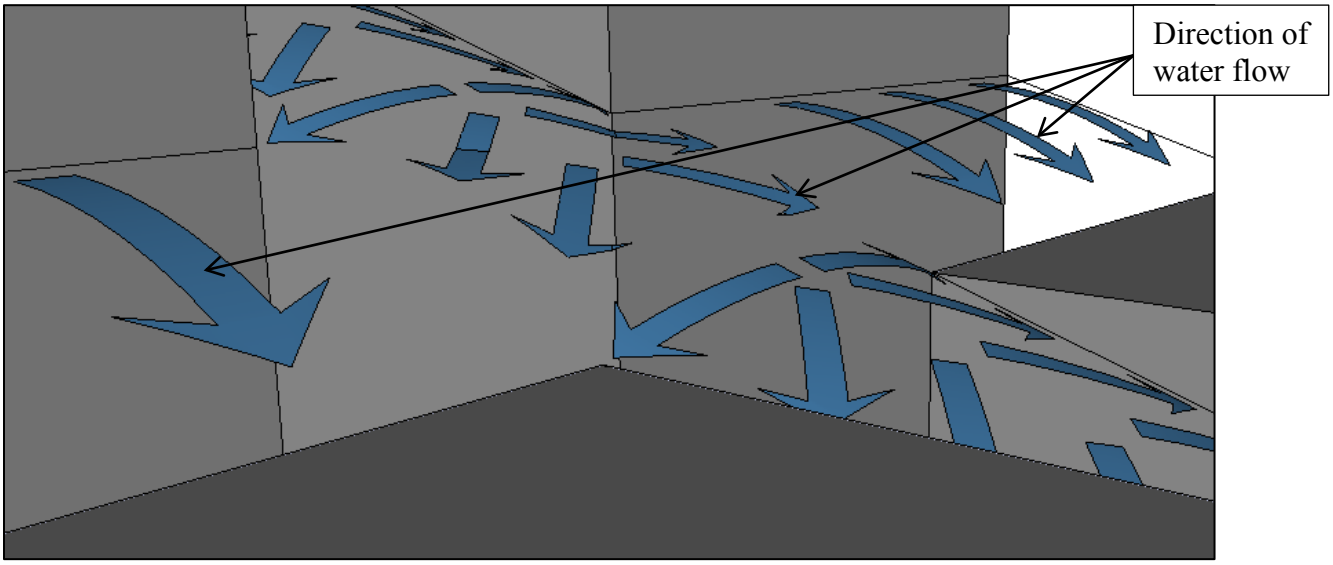

Figure 55: Close Up View of Crown in Roof for Water Drainage

4.3 Discarded Design Concepts

Previous designs would orient the cable truss orthogonally to the building's edge, instead of at 45 degrees. This inadvertently created awkward transition zones where cables had to be reoriented at 45 degrees between four buildings as shown in Figure 56. The change in cable orientation would create high point loads in the ETFE cushions.

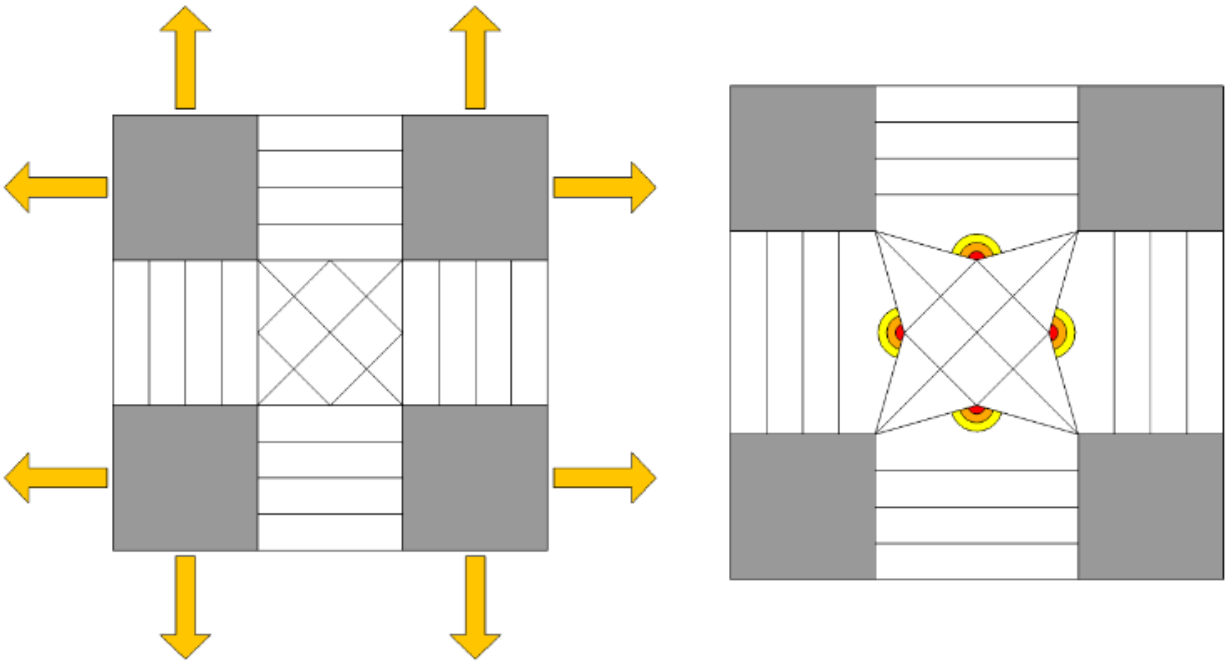

Figure 56: High Point Loads in ETFE from Cables

This design also posed a problem for the cables spanning between two neighboring buildings without any downhill component. This would result in ponding as shown in Figure 57.

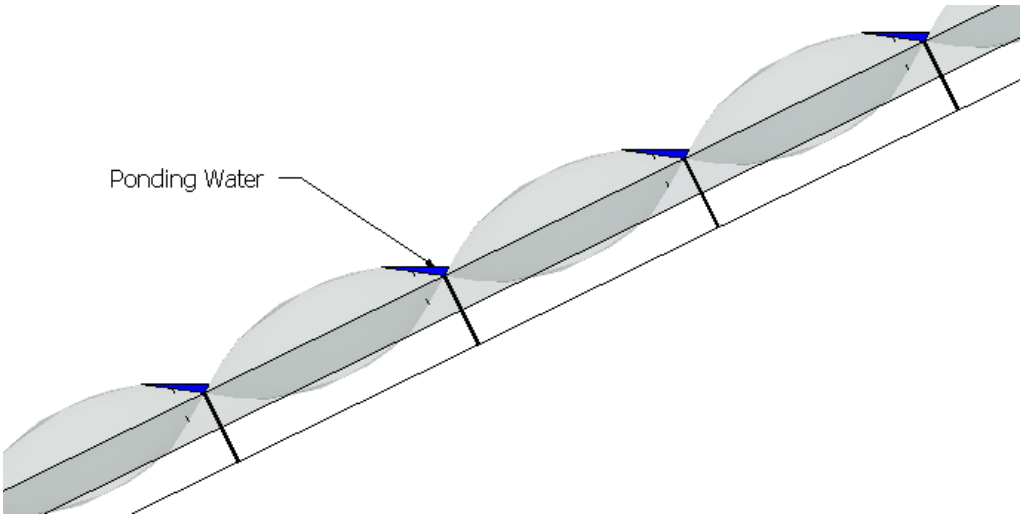

Figure 57: Ponding of Water Caused by ETFE Cushions

Other designs also considered not having a water collection system. Without this, water would accumulate down the slope of the roof and fall off the edge of the greenplex where city openings might be placed as illustrated in Figure 58.

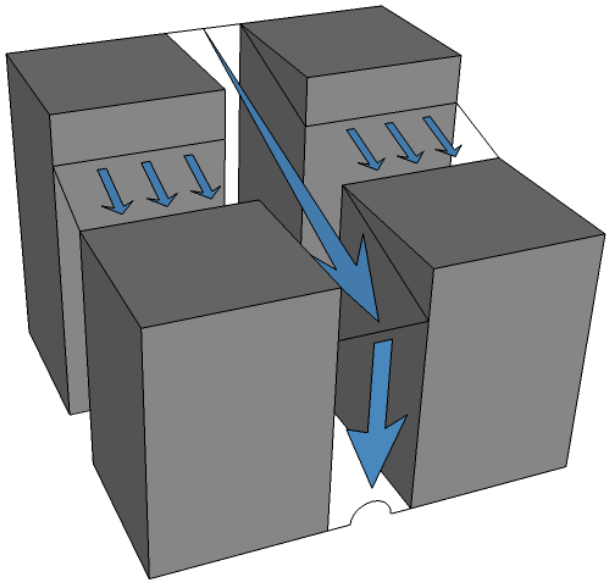

Figure 58: Uncollected Water Falling Off the Roof

Earlier designs attempted to find a cable topology that would direct all cables towards the buildings thus sending water towards the building gutters. All of these cable topologies had one thing in common, which is illustrated in Figure 59. The cable stresses are not resolved within the two skyscrapers they span between.

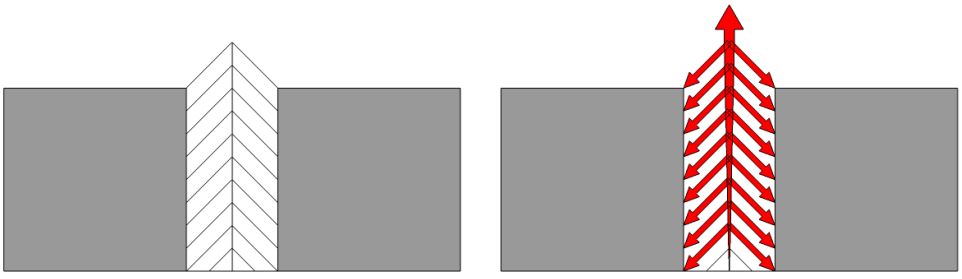

Figure 59: Unresolved Forces Between Buildings

Figure 59 shows that tensile forces propagate up the central cable and then have to be resisted by another building or support. This design approach would have compromised the roofs ability to accommodate for incremental greenplex construction. All cable forces accumulate two at a time up the central cables until they all apply their tensile load on the center building of the greenplex shown in Figure 60.

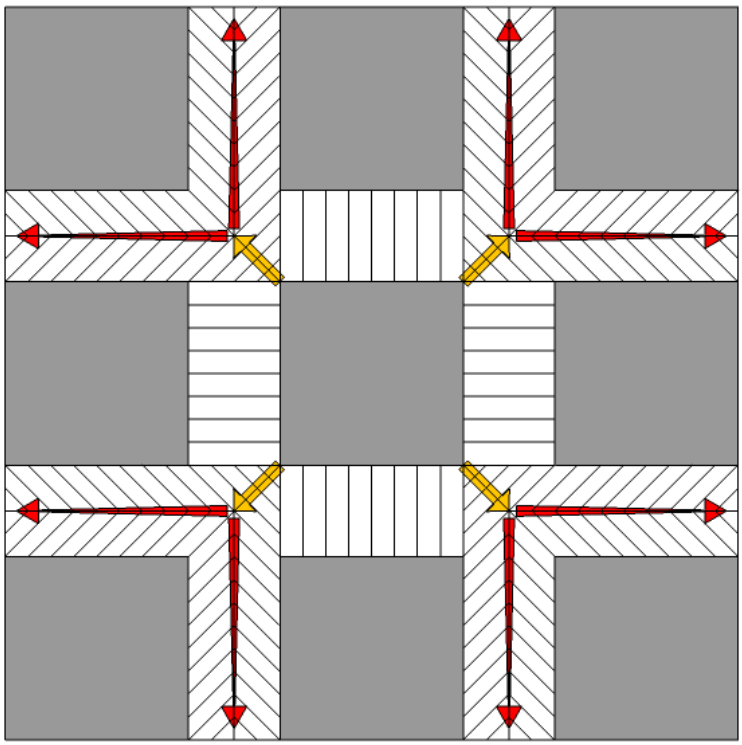

Figure 60: Cables all Apply Tension to the Center Building of Greenplex

Figure 61 shows that expanding the greenplex is difficult with this design because cable forces are added to the central cables that were not previously designed for.

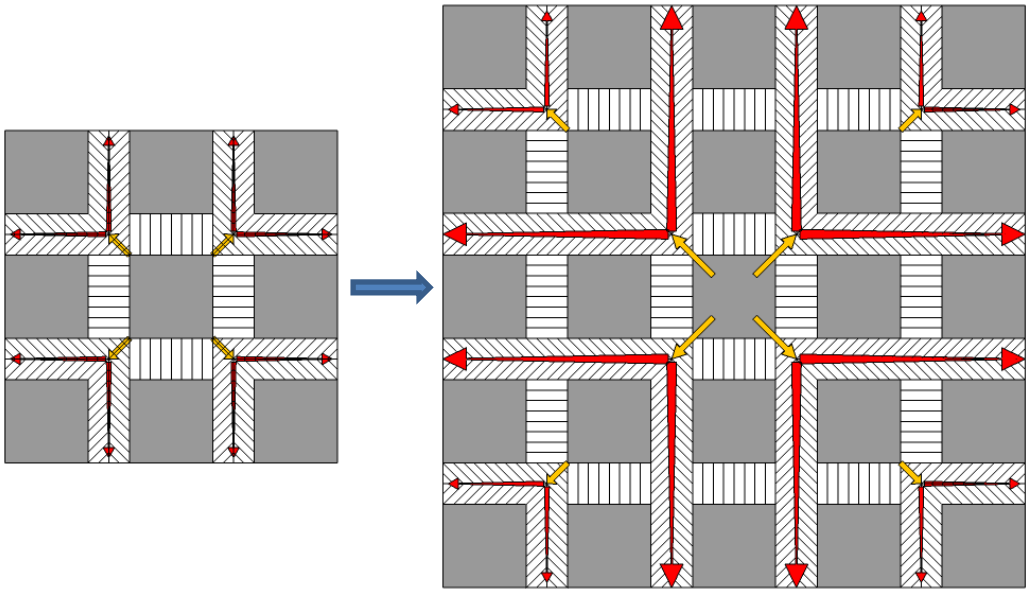

Figure 61: Expanding the Greenplex Results in Increase Cable Loads.

This greenplex roof design restricts city growth. Cables once designed for smaller loads now have to resist higher loads once another row of buildings is added to the perimeter.

5 DETAILED DESIGN AND ANALYSIS

The detailed analysis and design of the greenplex ETFE cushions and support system is described in this section. There are two components to the design of the greenplex atrium. The design of the triangular ETFE cushion marked in Figure 62 is described in Section 5.1. The design of the cable-spring truss in Figure 62 is described in Section 5.2. This cushion and truss were chosen since they experience the highest wind loads and support deflections in the system.

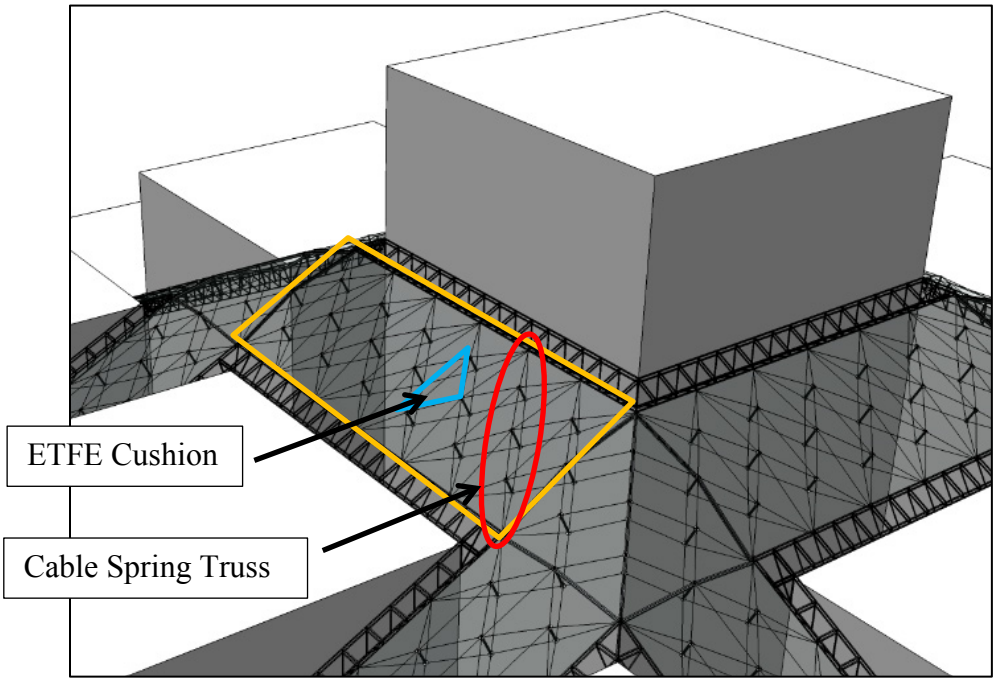

Figure 62: Triangular ETFE Cushion and Cable-Spring Truss to be Analyzed

5.1 ETFE Cushion Design

MPanel was used as an Auto CAD plugin to create the complicated geometry of the cushions, and to analyze it using dynamic relaxation to estimate stresses. Dynamic relaxation is a method of form finding and analysis for tensile structures. This approach traces the motion of a structure from the time of loading to when it reaches a position of equilibrium due to the effects of damping. Dynamic relaxation does not utilize an assembled structural stiffness matrix and hence is particularly suitable for highly nonlinear problems (Topping and Iványi 2007).

After wind loading analysis, it was determined that the top layer should consist of two vacuum sealed layers of 250 microns at 14% camber while the bottom layer will be a single layer of 250 microns at 17% camber. The design of the outer layers of foil was governed by wind suction while the bottom layer was governed by wind pressure. Figure 63 presents the final camber, thickness, and layering of the ETFE cushion.

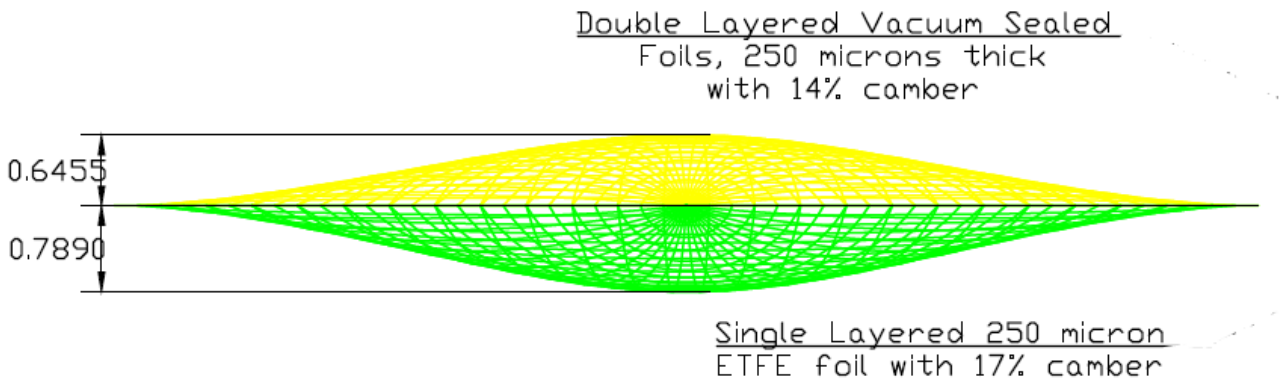

Figure 63: Front View of Final Cushion

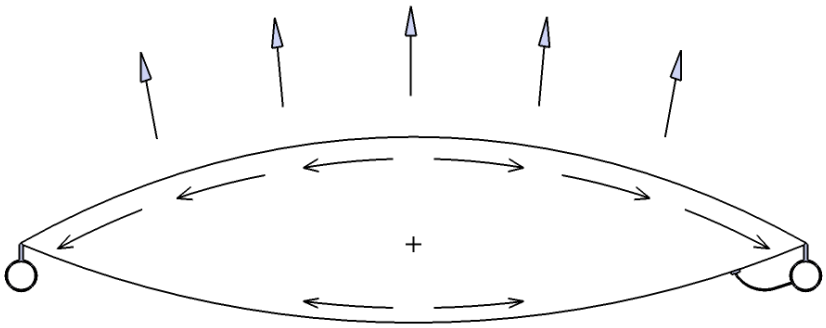

Figure 64: Top Layers are Governed by Wind Suction

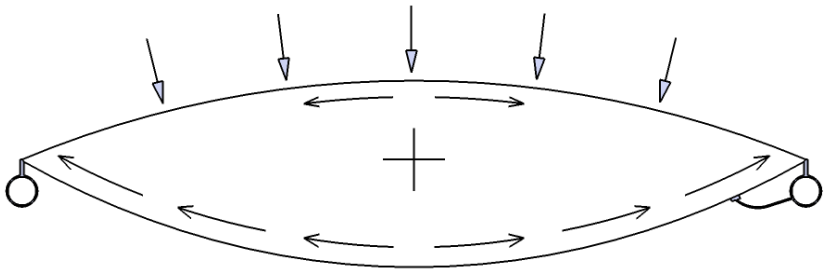

Figure 65: Bottom Layer is Governed by Wind Pressure

Maximum wind speeds were taken at 150 mph which produced loads of -4188 Pa and +1927 Pa in addition to the inflation pressure. The outer foils thus had to resist over twice the loads as the bottom foils. Increasing the camber of the outer foils is one way of relieving the stresses, but it can create lateral stability issues from cross wind loading. Most outer layers are never allowed to exceed 20% camber, and are regularly between 6-15%. Using this method alone to reduce the foil stresses would have been infeasible since the camber would have to be 27%. This could create very large oscillations under vortex shedding from high wind loads. Camber was thus reduced to 14% but was given added strength with a second ETFE foil to resist the load. The bottom layer was given a camber of 17% since no stability issues would exist on the greenplex interior. This increase in camber allowed the single bottom layer to more effectively resist positive wind loads without needing a second foil layer.

5.1.1 Creation of the Engineering Model

In order to create the inflated shape, the edges were meshed with 26 divisions in the warp and weft directions. Figure 66 shows the mesh size used from plan view. Figure 67 shows the mesh generated by MPanel for analysis and Figure 68 illustrates the element local x directions.

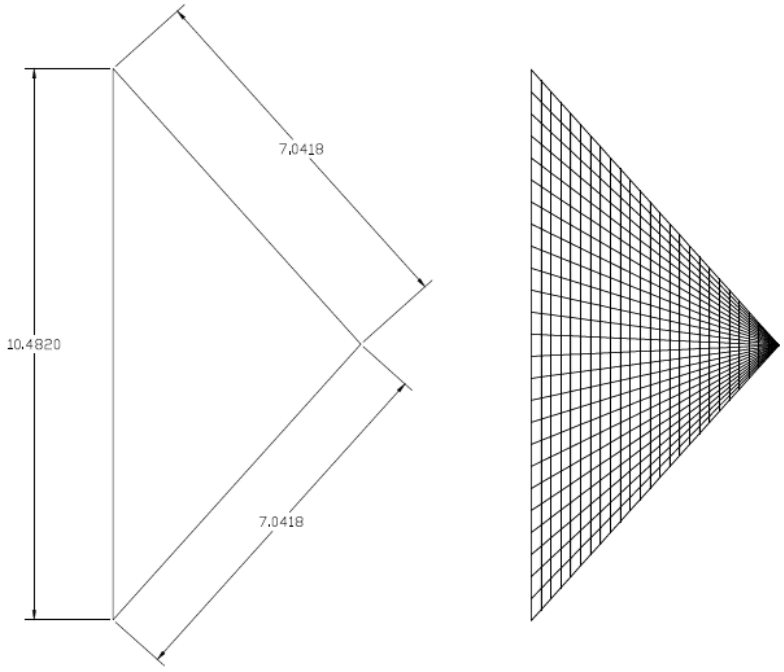

Figure 66: Cushion Dimensions in Meters and Mesh Size.

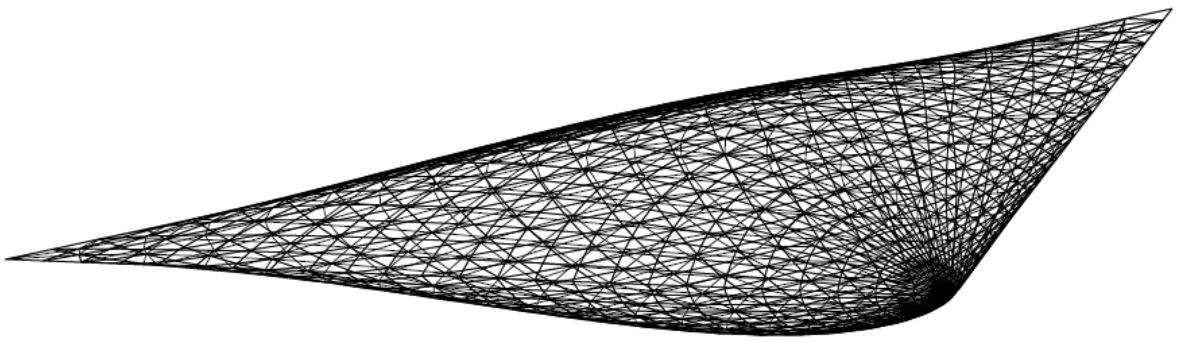

Figure 67: Generation of MPanel Mesh

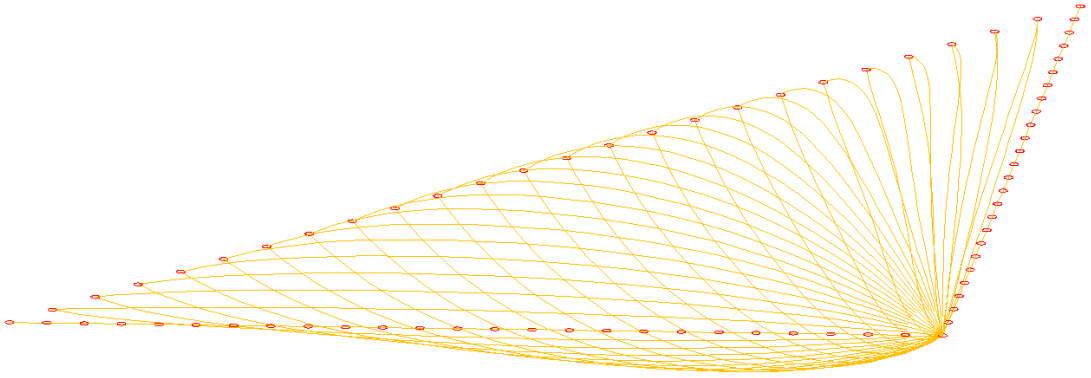

Figure 68: Local X Direction and Fixed Boundary Conditions

Table 4 shows the material properties of the ETFE used for analysis and Table 5 shows the properties for different membrane thicknesses.

Table 4: Assumed Material Properties

Property	Used in Calcs	Range	Units
Density	1.75	1.7 - 1.77	g/cm^3
Tensile Stiffness	750	300 - 1100	MPa
Shear Stiffness	75	30 -110	MPa
Poisson's Ratio	0.43	0.43 - 0.45	
Elastic Limit	16	14 - 20	MPa

Table 5: Material Properties for Each Foil Thickness.

Foil Thickness µm (microns)	Weight N/m^2	Ex N/m	Ey N/m	G N/m	UTSx N/m	UTSy N/m
50	0.85808	37500	37500	3750	800	800
100	1.71616	75000	75000	7500	1600	1600
150	2.57425	112500	112500	11250	2400	2400
200	3.43233	150000	150000	15000	3200	3200
250	4.29041	187500	187500	18750	4000	4000
300	5.14849	225000	225000	22500	4800	4800
350	6.00657	262500	262500	26250	5600	5600
400	6.86466	300000	300000	30000	6400	6400
450	7.72274	337500	337500	33750	7200	7200
500	8.58082	375000	375000	37500	8000	8000

The foil thicknesses greater than 350 microns are not true material properties since strength drops due to the brittle nature of thicker foils. This would have to be obtained from the manufacturer's tested results. However, foils greater than 350 microns were used to model double layers of thinner foils.

5.1.2 Prestressed State

The cushion was first analyzed under its prestressed state of 250 Pa of inflation. Notice that these stresses are quite low compared to the allowable 8000 N/m specified in Table 5. This permanent loading is also below the ETFE creep load of 2500 N/m.

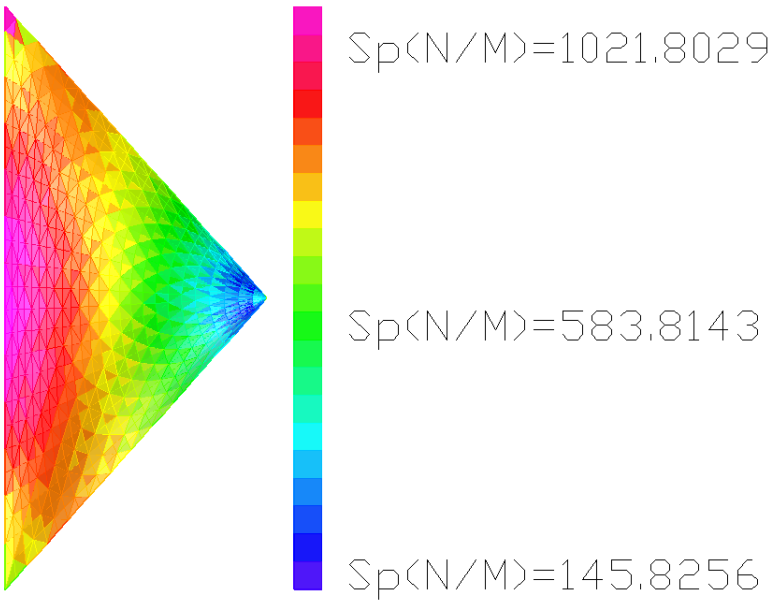

Figure 69: Stresses in Top Foils from Inflation

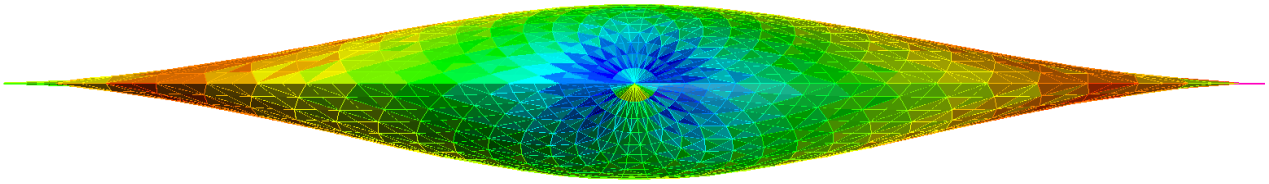

Figure 70: Front View of Cushion Under Inflation Pressure.

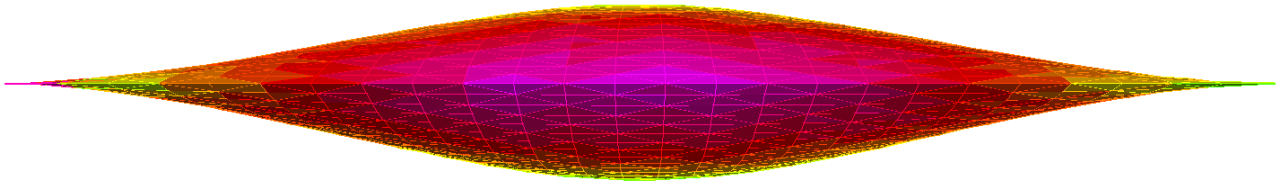

Figure 71: Back View of Cushion Under Inflation Pressure

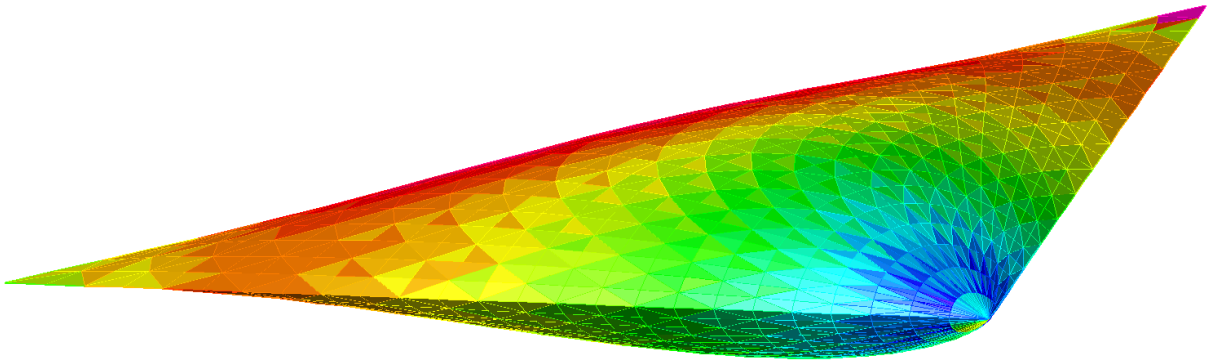

Figure 72: Isometric View of Cushion under Inflation Pressure

5.1.3 Wind Loads

Wind loads were obtained from the ASCE 7-05 wind load chapters (ASCE 2005). Table 6 shows the design pressures for the ETFE cushion with wind speeds of 150 mph.

Table 6: Wind Uplift and Pressure for Cushion Loading at 150 mph

Loading	Elevation (m)	q	GCp	qi	Gcpi	Pressure (psf)	Pressure (psf)
Wind Uplift	150	92.53	-0.9	92.53	0.18	**-87.48**	**-4188.77**
Wind Pressure	150	92.53	0.3	92.53	-0.18	**40.27**	**1927.92**

To predict the gradual buildup of stresses, the cushions were analyzed at a variety of wind speeds starting at 50 mph and incrementing up by 25 mph, to a maximum of 150 mph.

This produced a more complete understanding of the cushion performance. The analysis results are shown in Table 7 and Figures 73-75 show the stress analysis results from the 50 mph wind loads.

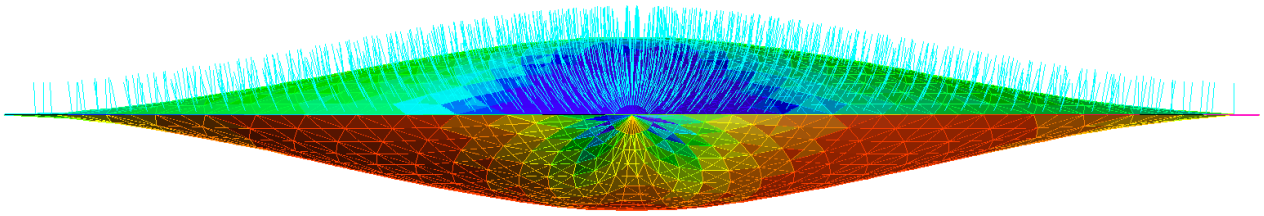

Figure 73: Front View of Cushion.

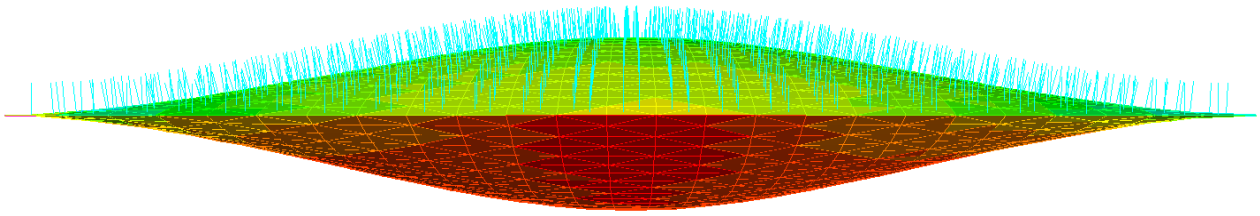

Figure 74: Back View of Cushion.

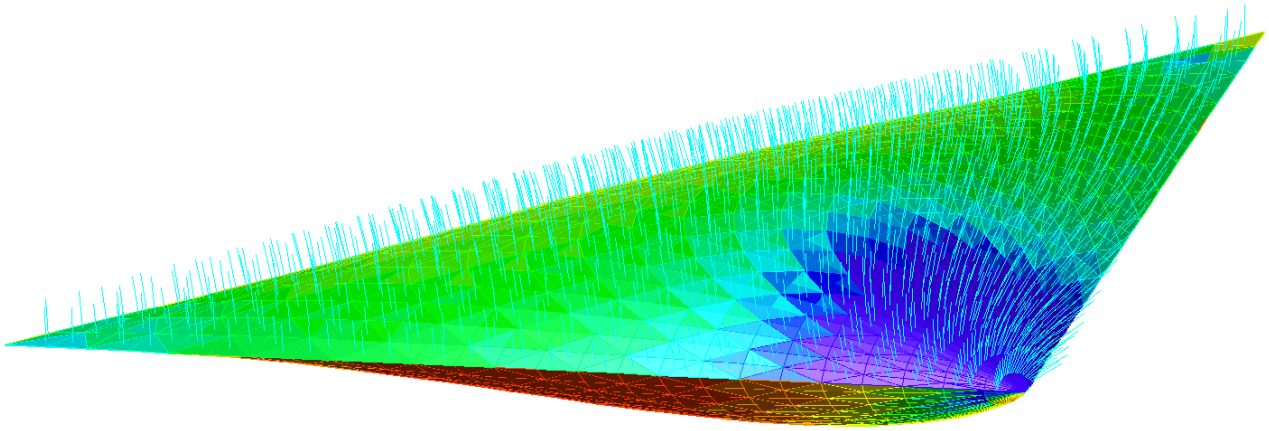

Figure 75: Isometric View of Cushion

Figures 76 and 77 show the results of the top and bottom layers under the highest wind loading of 150 mph. Large portions of the top and bottom foils undergo material nonlinearity under 150 mph winds. This however is not a problem due to ETFE's high ductility. Under such

loads the ETFE stretches, increasing its camber and material strength until the forces reach equilibrium again.

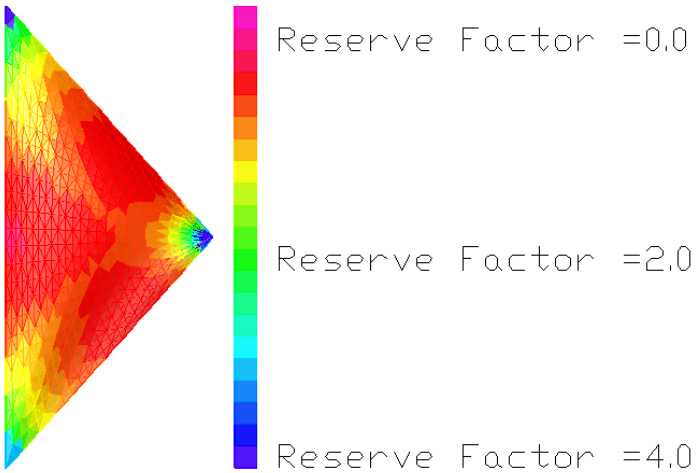

Figure 76: Factors of Safety for the Single Bottom Layer

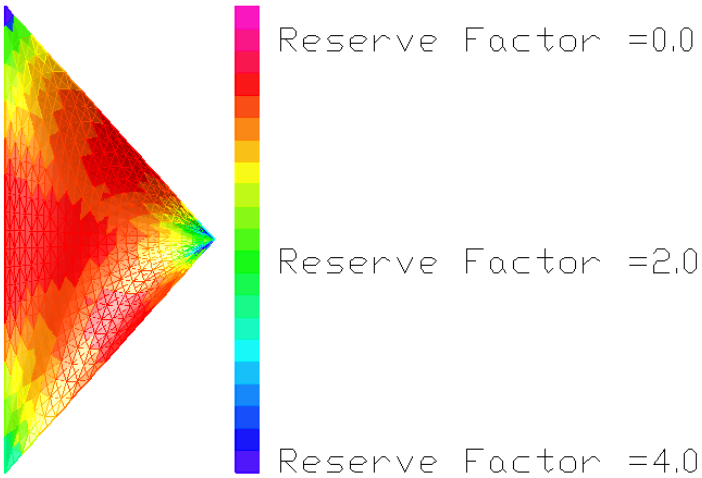

Figure 77: Factors of Safety for the Double Foil Top Layer

Modeling the ETFE cushions under material nonlinearity is rarely done analytically. These capabilities have not been deployed in MPanel because not enough testing has been done to determine pertinent material properties such as viscoelasticity, plasticity, and loading

hysteresis. ETFE designers often rely on empirical data from entire cushion tests. Attempting the same testing is beyond the scope of this thesis.

The cushion designs were fine-tuned so that both top and bottom foils would start to yield at wind speeds of 125 mph. This was accomplished by adjusting the number of foil layers, foil thicknesses, and camber. Table 7 presents the first principle stresses and factors of safety in the ETFE foils at various wind speeds. Note that material yielding for both top and bottom layers begins to occur at a wind speed of 125 mph.

Table 7: Material Factors of Safety at Various Wind Loads.

					Single Bottom Layer		Double Top Layer	
	Wind Speed		Pressure		Min Safety	Max Safety	Min Safety	Max Safety
Loading	mph	m/s	Pa	psf	Factor	Factor	Factor	Factor
Prestress State	0	0	250.00	5.22	3.92	25.98	6.76	51.07
Positive Pressure	50	22.35	464.21	9.70	3.17	14.27	-	-
	75	33.53	731.98	15.29	2.16	10.16	-	-
	100	44.70	1106.86	23.12	1.44	6.71	-	-
	125	55.88	1588.84	33.18	**1.02**	4.85	-	-
	150	67.06	2177.92	45.49	**Material Nonlinearity**	**Material Nonlinearity**	-	-
Negative Pressure	50	22.35	715.42	14.94	-	-	3.97	20.94
	75	33.53	1297.19	27.09	-	-	2.24	12.91
	100	44.70	2111.67	44.10	-	-	1.42	8.73
	125	55.88	3158.87	65.97	-	-	**1.00**	7.04
	150	67.06	4438.77	92.71	-	-	**Material Nonlinearity**	**Material Nonlinearity**

5.2 Cable-Spring Truss Design

While relevant and valuable work was accomplished on the ETFE cushion design the detailed design of the cable-spring truss is the major contribution of this thesis. The cross section of a cable-spring truss is shown in Figure 78. The span and depth are defined to be the horizontal and vertical dimensions of the truss. Note that the depth is essentially the depth of the spring in the center of the truss. It is assumed that the depth of the secondary springs located at the quarter points is always 75% of the depth of the center spring.

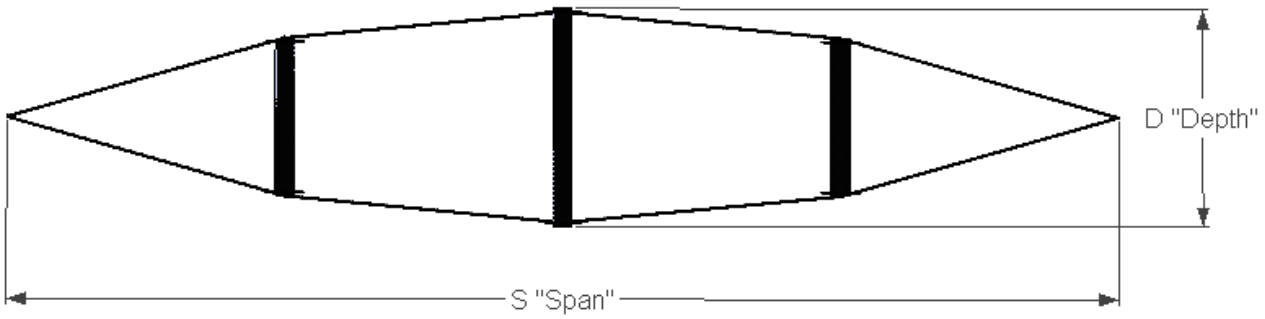

Figure 78: Cable-Spring Truss Cross Section and Variable Names

The cable-spring truss was designed and analyzed in the following five steps: 1) determine minimum and maximum spans (Section 5.2.1); 2) design minimum and maximum depths (Section 5.2.2); 3) design spring constants (Section 5.2.3); 4) design cable cross-section areas (Section 5.2.4), and 5) determine the weight and support reactions exerted on the buildings (Section 5.2.5).

5.2.1 Maximum and Minimum Spans

Building displacements and rotations produce expansions and contractions of the cable-spring trusses. This is illustrated in Figure 79 with one edge of building 1 displacing up and the adjacent edge on building 2 displacing down, which creates expansion in the cable-spring support system spanning between buildings 1 and 2. Figure 79 also illustrates that the cable-spring support system spanning between buildings 1 and 3 contracts.

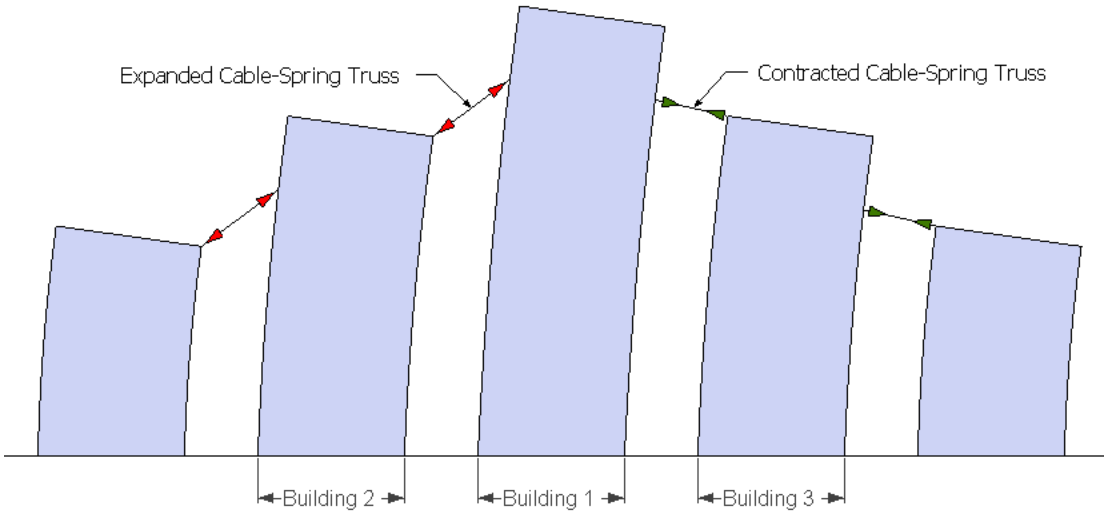

Figure 79: Expansion and Contractions in Roof

The buildings of the greenplex were optimized and analyzed under wind and seismic loads without the ETFE atria to obtain displacements at points A, B, C, D, E, and F which are labeled on Figure 80.

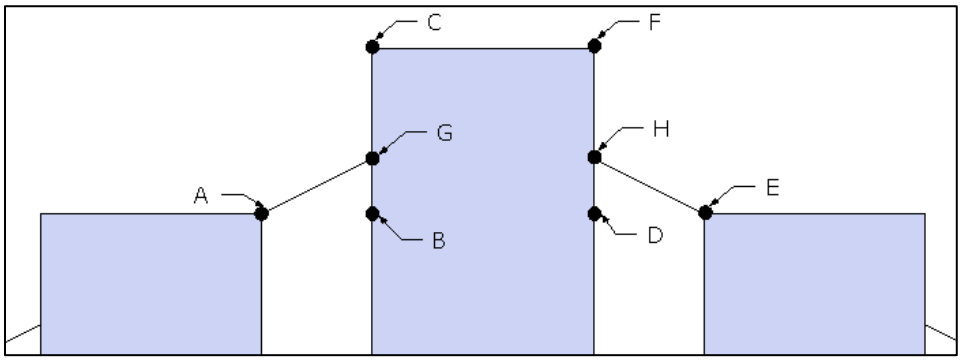

Figure 80: Points Indicate Where Displacements Were Measured or Interpolated

The displacements at point G were determined by interpolating between points B and C while H was interpolated between points F and D. The displacements at points A, G, E, and H were used to calculate the expanded and contracted spans between the buildings as shown in Table 8. These spans are orthogonal to the building edges.

Table 8: Orthogonal Spans for Wind and Seismic

	System Span bw A and G (m)	
Truss State	Wind	Seismic
Expanded	20.9874	**21.0485**
Contracted	20.9389	**20.8777**

Recognizing that the cable-spring truss is oriented at 45 degrees between the building edges means that trigonometry can be used to solve for the expanded and contracted lengths of the truss. These spans are shown in Table 9.

Table 9: Truss Spans for Wind and Seismic

	Cable-Spring Truss Span (m)	
Truss State	Wind	Seismic
Expanded	29.6635	**29.7068**
Contracted	29.6292	**29.5860**

5.2.2 Maximum and Minimum Depths

This section designs the springs to have sufficient depth to allow for the expansion and contraction requirements found in Table 9. These are also used to determine the uncompressed length of the springs and the length of the telescoping tubes. The governing displacements are produced by seismic loading which are highlighted in Table 9. Let $S_1 = 29.7068\,m$ be the maximum span from Table 9, and let $S_2 = 29.5860\,m$ be the minimum span from Table 9. Let D_1 and D_2 equal the depths of the center springs at states 1 and 2. Figure 81 shows the spans and depths corresponding to these expanded and contracted states.

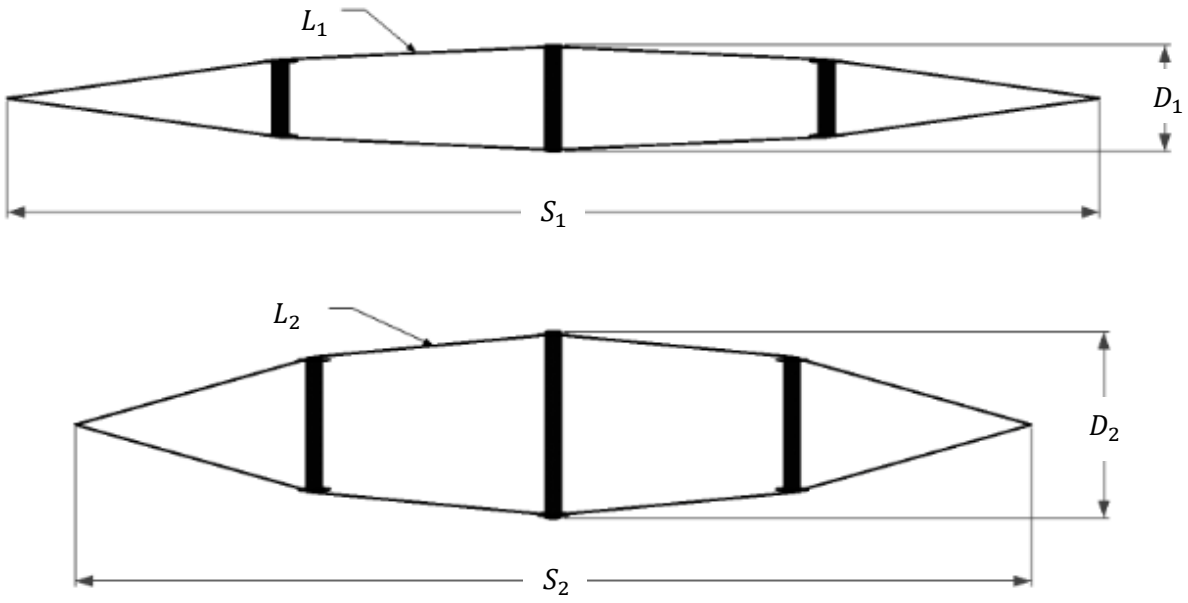

Figure 81: Variable Names

L_1 and L_2 are the lengths of the cables which must be equal between these two states. Equating L_1 and L_2 in terms of spans and depths yields Equation 5-1.

$$2 * \left(\sqrt{\left(\frac{S_1}{4}\right)^2 + \left(\frac{0.75 * D_1}{2}\right)^2} + \sqrt{\left(\frac{S_1}{4}\right)^2 + \left(\frac{0.25 * D_1}{2}\right)^2} \right)$$

Equation 5-1

$$= 2 * \left(\sqrt{\left(\frac{S_2}{4}\right)^2 + \left(\frac{0.75 * D_2}{2}\right)^2} + \sqrt{\left(\frac{S_2}{4}\right)^2 + \left(\frac{0.25 * D_2}{2}\right)^2} \right)$$

This leaves one equation and two unknowns which are D_1 and D_2. These can be reduced to one unknown by specifying the value of a design variable "R". This is given in Equation 5-2 and shown in Figure 82. An engineer would choose R to describe the range of spring displacement between the critical states.

$$R = \frac{D_1}{D_2}$$

Equation 5-2

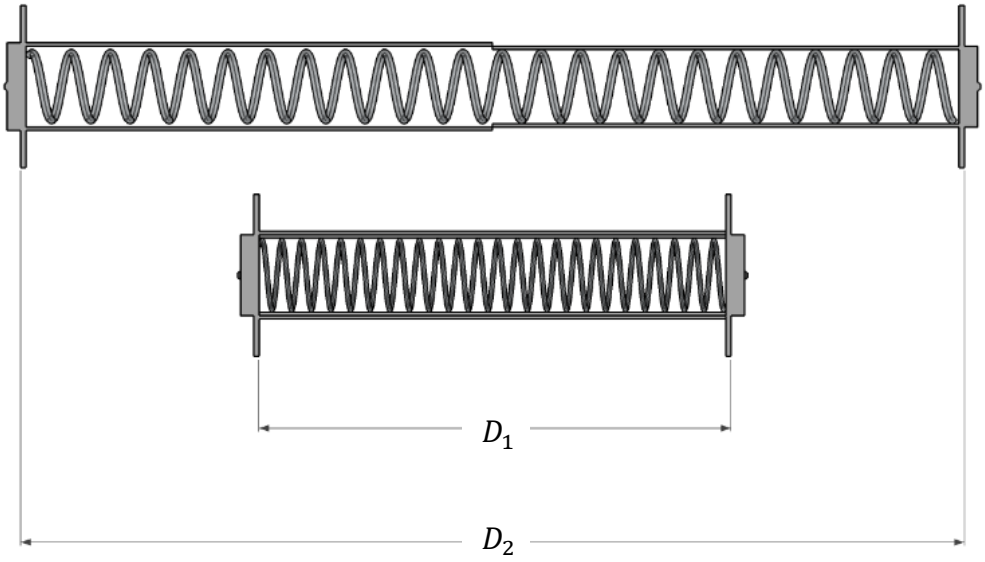

Figure 82: Variables Used to Define R

Figure 82 illustrates the case of R = 0.5. Note that in the expanded position, the two telescoping tubes are on the verge of separating one from another. In the compressed position, the two telescoping tubes are in contact with the end caps. To allow for additional expansion and contraction it is recommended to use R values higher than 0.5.

Substituting Equation 5-2 into Equation 5-1 gives us Equation 5-3.

$$2 * \left(\sqrt{\left(\frac{S_1}{4}\right)^2 + \left(\frac{0.75 * R * D_2}{2}\right)^2} + \sqrt{\left(\frac{S_1}{4}\right)^2 + \left(\frac{0.25 * R * D_2}{2}\right)^2} \right) \quad \textbf{Equation 5-3}$$

$$= 2 * \left(\sqrt{\left(\frac{S_2}{4}\right)^2 + \left(\frac{0.75 * D_2}{2}\right)^2} + \sqrt{\left(\frac{S_2}{4}\right)^2 + \left(\frac{0.25 * D_2}{2}\right)^2} \right)$$

Solving for D_2 using Mathematica and choosing the correct root gives us Equation 5-4.

$$D_2 = 0.5\left[2\left[\frac{\left(-20{S_1}^2R^4 + 40{S_1}^2R^2 - 20{S_1}^2 - 20{S_2}^2R^6 + 40{S_2}^2R^4 - 20{S_2}^2R^2\right)^2}{(4R^8 - 25R^6 + 42R^4 - 25R^2 + 4)^2}\right.\right.$$

$$\left. - \frac{4\left(16{S_1}^4 - 16{S_1}^2{S_2}^2R^4 - 16{S_1}^2{S_2}^2 + 16{S_2}^4R^4\right)}{4R^8 - 25R^6 + 42R^4 - 25R^2 + 4}\right]^{\frac{1}{2}}$$

$$\left. - \frac{2\left(-20{S_1}^2R^4 + 40{S_1}^2R^2 - 20{S_1}^2 - 20{S_2}^2R^6 + 40{S_2}^2R^4 - 20{S_2}^2R^2\right)}{4R^8 - 25R^6 + 42R^4 - 25R^2 + 4}\right]^{\frac{1}{2}}$$

Equation 5-4

Figure 83 graphs Equation 5-4 and also normalizes D_2 with S_1 so that it can be used for any roof expansion and contraction requirements.

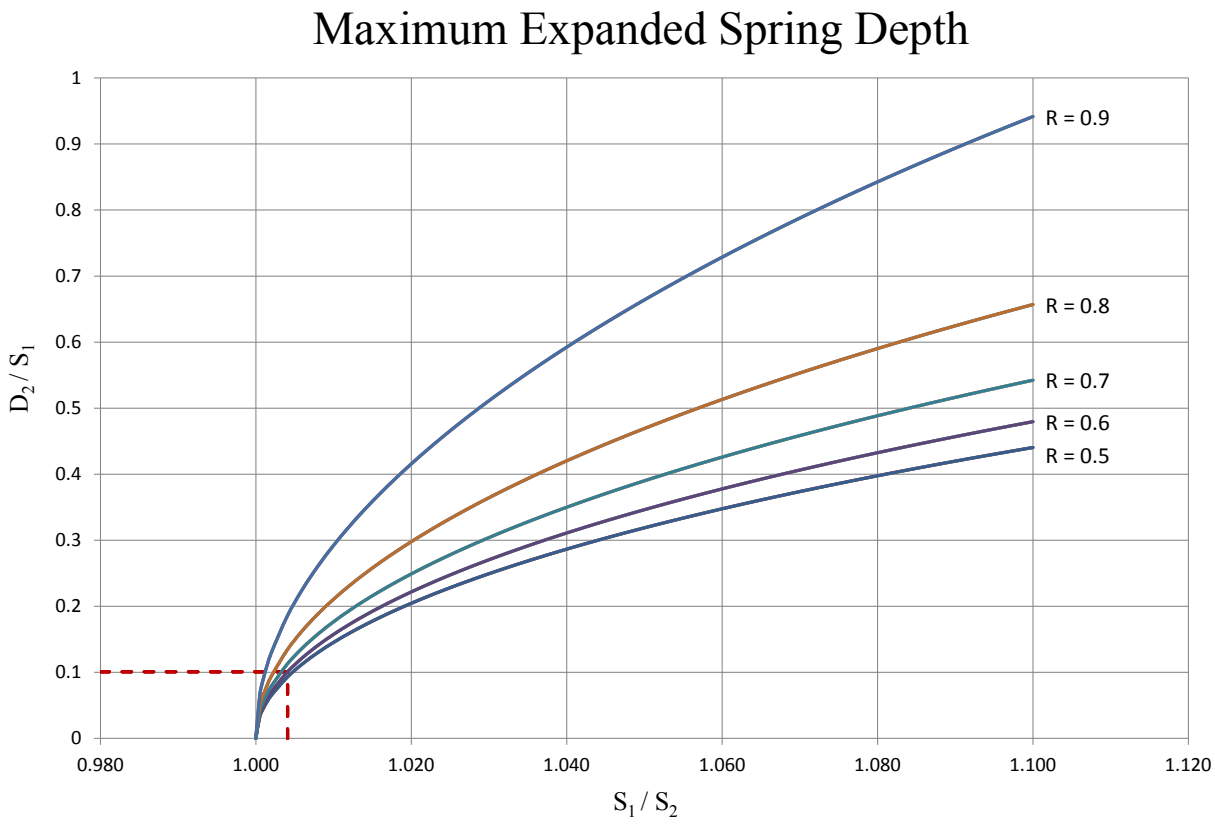

Figure 83: Design Guide to Determine the Uncompressed Spring Depth

An R value of 0.6 was used to obtain a depth of 3 m for D_2 and 1.8 m for D_1. The length of the telescoping tubes was also calculated to make sure that the tubes do not collapse or separate prematurely under seismic expansion and contraction. Equation 5-5 shows the range of acceptable tube lengths.

$$\frac{D_2}{2} \leq T \leq D_1$$ **Equation 5-5**

Where:

T = the length of a single tube as shown in Figure 84

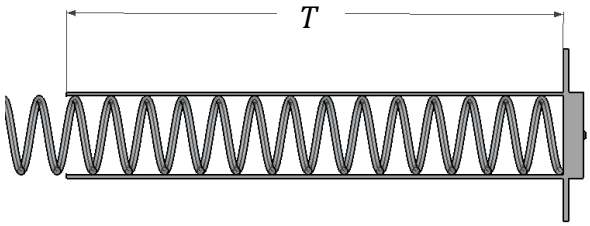

Figure 84: Length of a Single Telescoping Tube

Equation 5-6 calculates T and ensures that the gap in the compressed state equals the overlap in expanded state. Figure 85 helps illustrate this.

$$T = \frac{D_1 + D_2}{3}$$ **Equation 5-6**

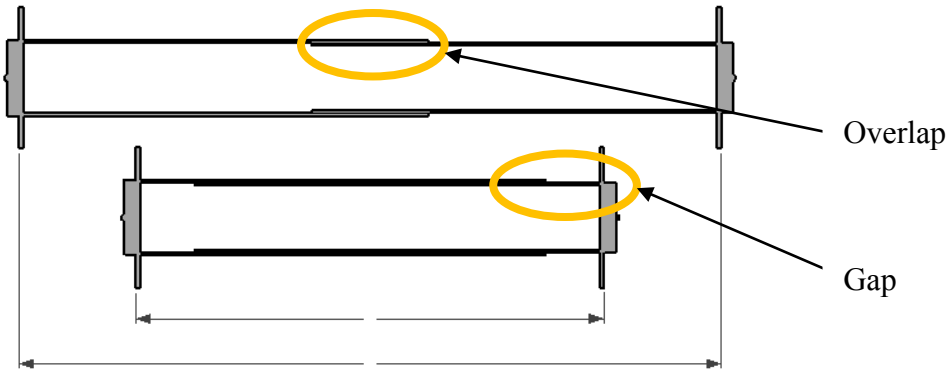

Figure 85: Gap and Overlap of Tubes

Equation 5-6 gives this design a tube length of 1.6 m. Calculating the uncompressed spring depth is now accomplished by relating the tube lengths to the spring depth as shown in Equation 5-7.

$$D_0 = 2 * T$$ **Equation 5-7**

This gives us an uncompressed spring depth of $D_0 = 3.2$ m. With the depths and spans known for both states 1 and 2, the cable length is calculated to be 29.775 m using one side of Equation 5-3. Using Equation 5-8, the depth of the center spring (D) can be calculated for any span (S) if the designer also knows the cable's length (L).

$$D = \frac{\sqrt{5L^2 - \sqrt{L^2(9L^2 + 16S^2)}}}{\sqrt{2}}$$ **Equation 5-8**

Using Equation 5-8 allows us to calculate the depth of the springs during wind expansion and contraction shown in Table 9. Table 10 reports all of the center spring depths of during seismic, wind, and service loads.

Table 10: Spring Depths at Wind and Seismic Loading

	Spring Depth (m)	
Spring State	Wind	Seismic
Contracted	2.30	**1.80**
Service	2.47	2.47080
Expanded	2.63	**3.00**

5.2.3 Spring Constant

Now that the spring depths are determined, the spring stiffnesses are required to solve for cable loads and building reactions. The stiffness of the springs can be somewhat arbitrary but must maintain stability under wind loads. Choosing a low spring stiffness results in small support reactions on the buildings, but may result in the structure becoming unstable or not

complying with service or aesthetic requirements. This situation may arise when the support locations don't change substantially but there is significant wind pressure that makes the springs compress and the cables go slack as illustrated in Figure 86.

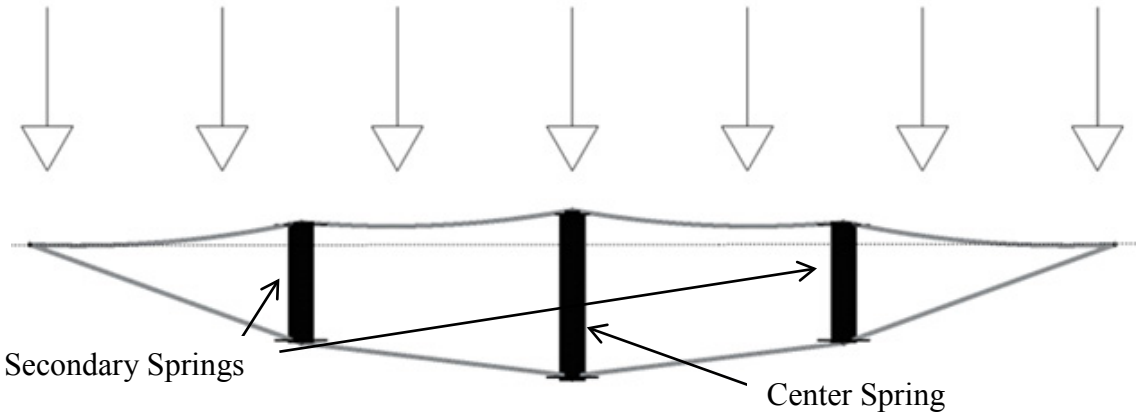

Figure 86: Predicted Shape of Truss under Evenly Distributed Wind Pressure

Increased spring stiffness reduces the amount of deflection and the amount of sag in the cables. The wind speed the springs were designed to resist was 75 mph. Under the short term wind gusts of 150 mph it is not needful for the structure to comply with such strict service or aesthetic requirements. In other words, the springs were designed to have sufficient stiffness to resist a sustained wind load of 75 mph before the telescoping tubes contact the end caps. This design allows for much lower spring and cable loads, and ultimately lower building reactions. Equation 5-9 was used to calculate the stiffness of the center spring.

$$K_c = \frac{A_T * P_{wind}}{\delta_c} \qquad \textbf{Equation 5-9}$$

Where:

$\delta_c = Center\ spring\ deflection$

$A_T = Tributary\ wind\ area\ per\ spring$

$P_{wind} = Wind\ pressure$

$K_c = Stiffness\ of\ center\ spring$

Using a wind pressure of 482 Pa, a tributary area for each spring of 49.5 m^2 and a deflection requirement of 1.6 m provides a spring stiffness of 14,912 N/m as shown in Equation 5-10.

$$K_c = \frac{49.5m^2 \ * 482 \text{ Pa}}{1.6\, m} = 14{,}912/m$$ **Equation 5-10**

The springs were designed to exert the same forces into the cables at every deflected truss shape. Since the two secondary springs collapse less than the center spring during roof expansion, they must be stiffer. The expressions below quantify how stiff the secondary springs need to be. This is done by using the deflections that the center spring and the two secondary springs experience between states 1 and 2. Equations 5 – 11 and 5 – 12 calculate these forces.

$$F_c = K_c * \delta_c$$ **Equation 5-11**

$$F_s = K_s * \delta_s$$ **Equation 5-12**

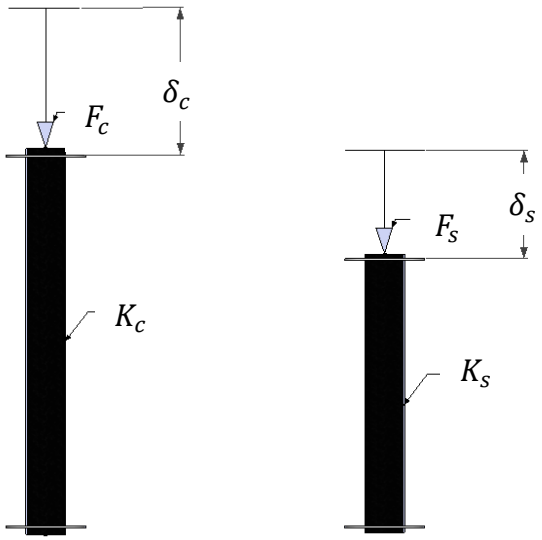

Figure 87: Statics Used to Determine K_s

Where:

$F_c = The\ force\ in\ the\ center\ spring$

$F_s = The\ force\ in\ the\ secondary\ spring$

$\delta_s = The\ deflection\ in\ the\ secondary\ spring$

Now letting $F_s = F_c$, gives us Equations 5-13 through 5-16.

$$K_c * \delta_c = K_s * \delta_s \quad \textbf{Equation 5-13}$$

$$K_s = K_c * \frac{\delta_c}{\delta_s} \quad \textbf{Equation 5-14}$$

$$K_s = K_c * \frac{1.2m}{0.9m} \quad \textbf{Equation 5-15}$$

$$K_s = \frac{4}{3} * K_c \quad \textbf{Equation 5-16}$$

Equation 5-16 shows the outer springs must be 4/3 as stiff as the center springs in order for all spring forces to be equivalent. This stiffness ratio is also the inverse of the length ratios which is 3/4. Using these results gives a center spring stiffness of $14{,}912\ N/m$ and a secondary spring stiffness of $19{,}883\ N/m$.

5.2.4 Cable Cross Sectional Areas

Gross cross sectional areas of steel are calculated for the cables in this section. Three load cases were considered in the design of the cables:

1. Seismic Displacement
2. Wind Expansion and Pressure
3. Wind Contraction and Suction

Four cable sections were size optimized with the recommended factor of safety of 2.2 according to ASCE 19-10 (ASCE 2010b). These cables are shown in Figure 88 and are grouped in this manner because stresses in these cables are nearly identical.

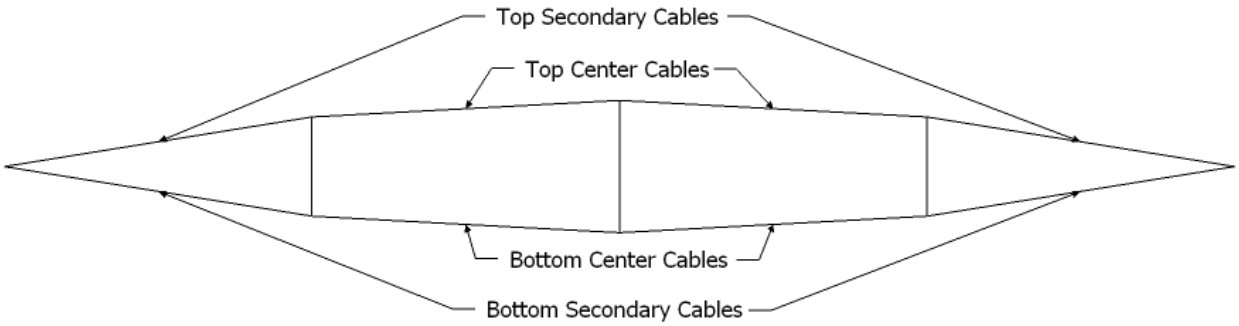

Figure 88: Four Types of Cables to be Size Optimized.

The design strength of the cables is taken to be 270 ksi. The principles of statics were employed to solve for cable forces using Figures 89 and 90 and Equations 5-17 and 5-18.

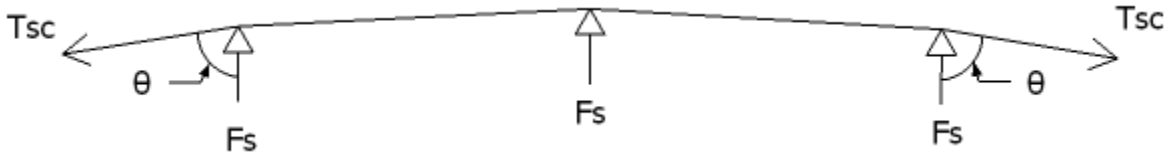

Figure 89: Free Body Diagram for Tensions in the Secondary Cables

$$T_{sc} = \frac{3 * F_s}{4 * \cos(\theta)}$$ **Equation 5-17**

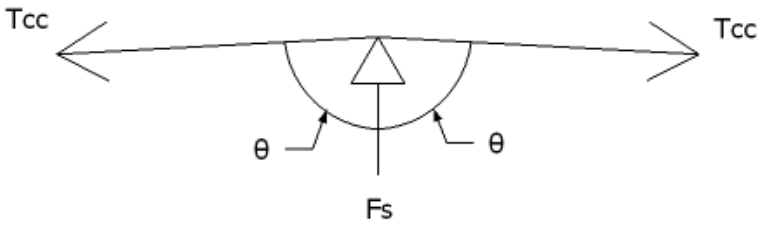

Figure 90: Free Body Diagram for Tensions in the Center Cables

$$T_{cc} = \frac{F_s}{4 * \cos(\theta)}$$ **Equation 5-18**

In Equations 5-17 and 5-18 the axial force in the cables is divided by 4 due to the four cables at each joint as shown in Figure 91. Loads for these various cable groupings are shown in Tables 11 and 12. Required areas of steel are calculated in presented in Table 13.

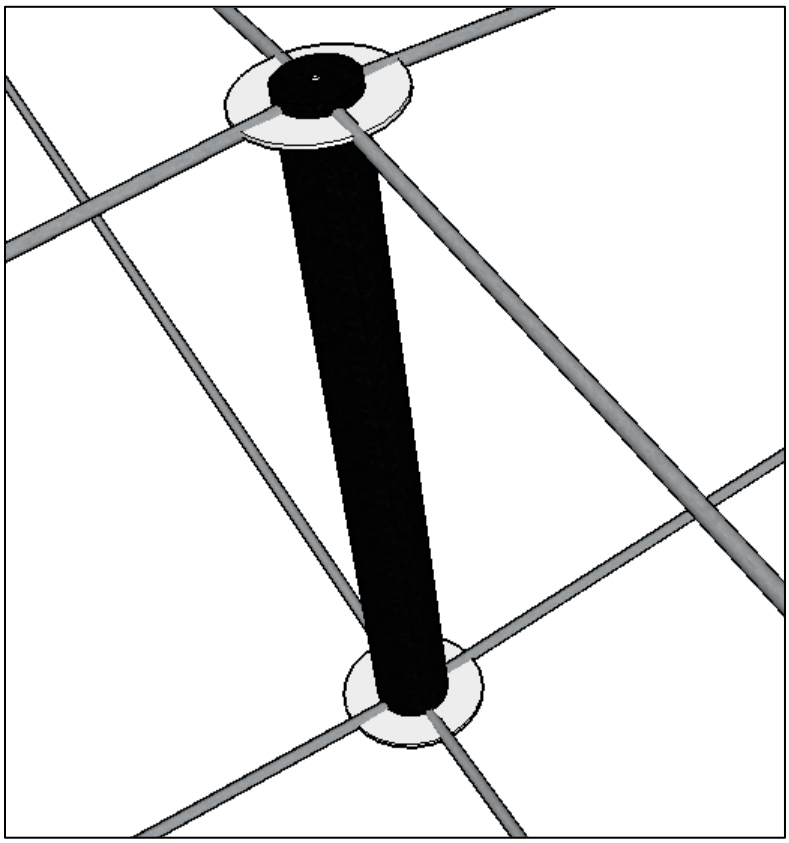

Figure 91: Four Cables that Intersect at Both Top and Bottom of Springs

Table 11: Loads in the Cables in kN

	Axial Forces In Cables (kN)										
	Positive Wind Pressure				Wind Uplift Loading			Seismic Loading			Maximum
Cables Analyzed	Springs	Wind Pressure	Dead Weight	Total	Springs	Wind Pressure	Total	Springs	Dead Weight	Total	Loading
Top Secondary	-	-	-	-	24.52	797.98	**822.50**	87.54	-	87.54	**822.50**
Top Center	-	-	-	-	23.79	774.12	**797.91**	86.29	-	86.29	**797.91**
Bottom Secondary	44.20	417.31	3.47	**464.99**	-	-	-	87.54	4.80	92.34	**464.99**
Bottom Center	43.18	407.68	3.43	**454.30**	-	-	-	86.29	4.77	91.07	**454.30**

Table 12: Loads in the Cables in kips

	Axial Forces In Cables (kip)										
	Positive Wind Pressure				Wind Uplift Loading			Seismic Loading			
Cables Analyzed	Springs	Wind Pressure	Dead Weight	Total	Springs	Wind Pressure	Total	Springs	Dead Weight	Total	Maximum
Top Secondary	-	-	-	-	5.51	179.39	**184.91**	19.68	-	19.68	**184.91**
Top Center	-	-	-	-	5.35	174.03	**179.38**	19.40	-	19.40	**179.38**
Bottom Secondary	9.94	93.82	0.78	**104.53**	-	-	-	19.68	1.08	20.76	**104.53**
Bottom Center	9.71	91.65	0.77	**102.13**	-	-	-	19.40	1.07	20.47	**102.13**

Table 13: Required Areas of Steel

Cables Designed	Area of Steel (in^2)	Factor of Safety
Top Secondary	1.51	2.20
Top Center	1.46	2.20
Bottom Secondary	0.85	2.20
Bottom Center	0.83	2.20

Tables 11 and 12 show that the governing loads for the top and bottom cables are wind uplift and positive wind pressure. Loads from the springs, wind loads, and gravity loads were taken separately and superimposed for a total axial force in the cables. Note that the loads in the cables caused by the springs and dead weight are substantially less than the loads caused by wind.

Wind loads are the same loads used in 5.1.3 when designing the ETFE cushions. Wind forces from pressure and uplift were lumped into point loads through the springs. This is shown in Figure 92. Figure 93 illustrates the locations of wind pressure and uplift in relation to wind direction as well as the current shape of the trusses during loading.

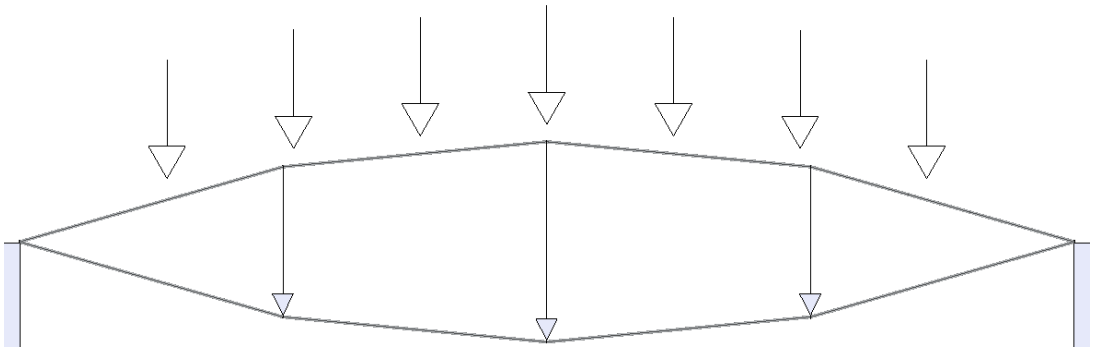

Figure 92: Distributed Wind Loads Transformed into Point Loads.

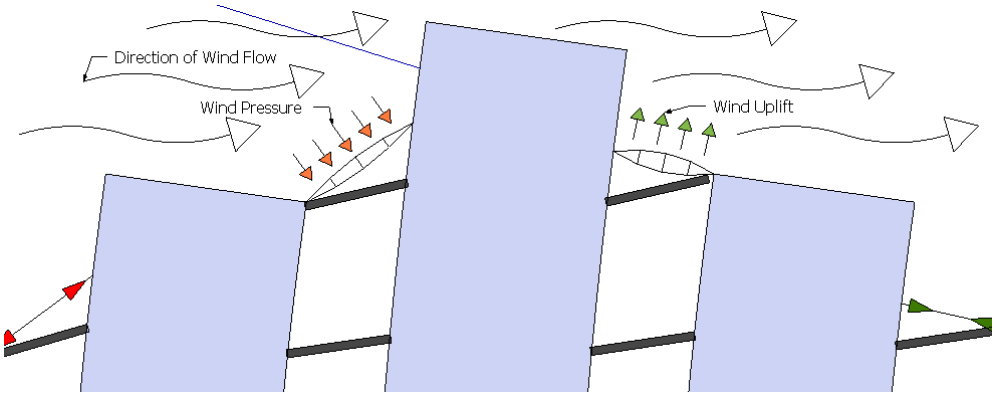

Figure 93: Locations of Wind Pressure and Wind Uplift

5.2.5 Building Reactions and Weight

The building reactions caused by building displacements are calculated in this section. Only one connection point was analyzed as shown in Figure 94. The reaction parallel to the truss span was calculated as shown in Figure 95.

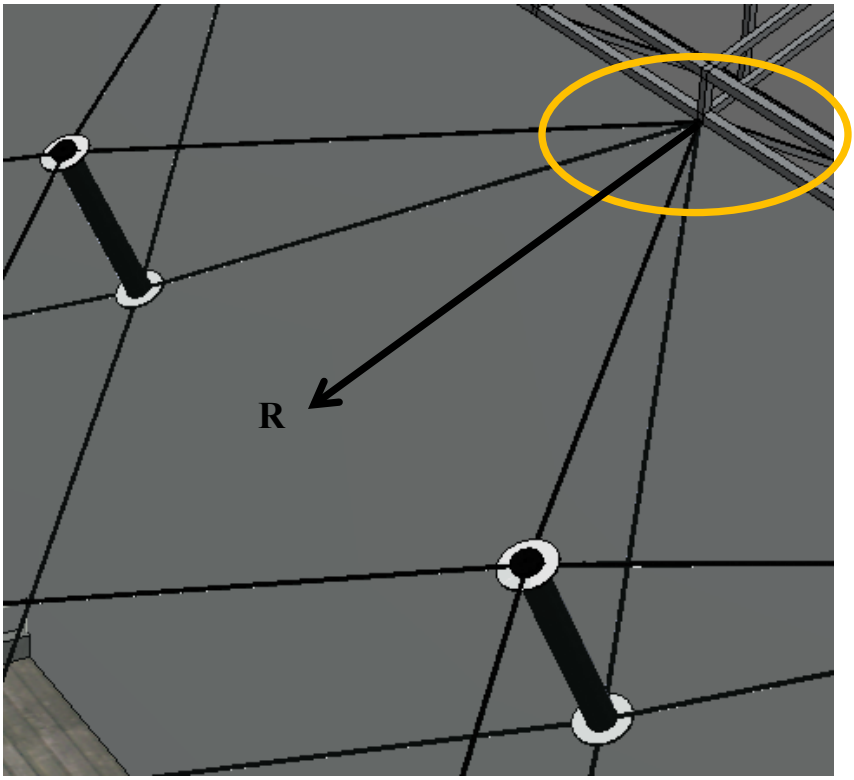

Figure 94: Connection to be Analyzed for Building Reactions

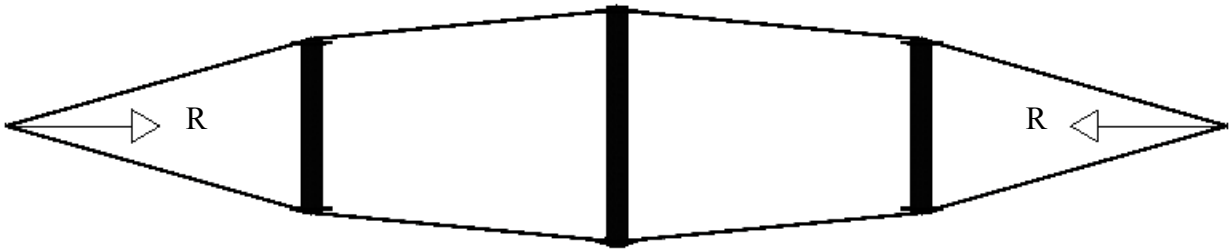

Figure 95: Reaction R on Support Connections

Figure 96 plots the support reactions of the connection shown in Figure 94 for seismic and wind displacements. The x axis measures the positive and negative displacements from the

roof's service span. Positive values represent expansion and negative values represent contraction. Notice that the largest displacements and support reactions occur under seismic expansion.

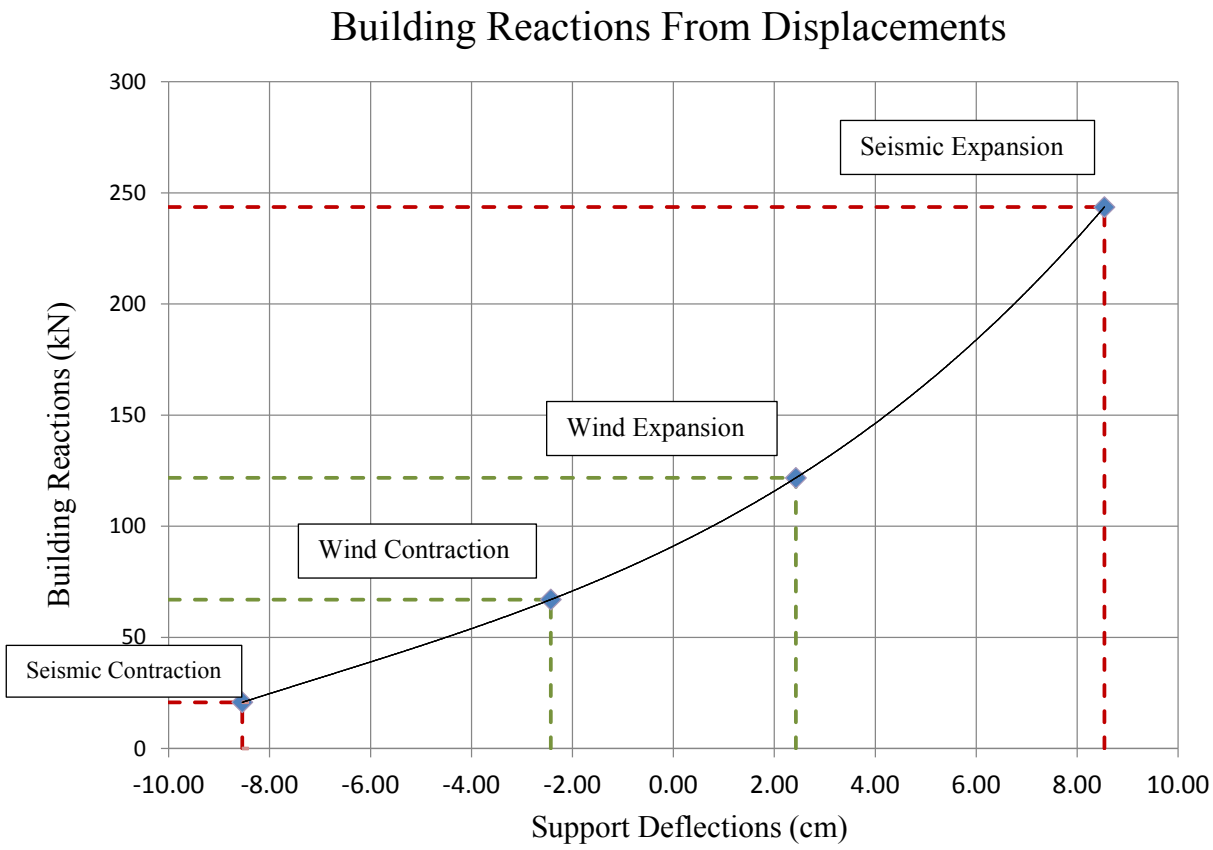

Figure 96: Tension in Secondary Cables due to Support Movements

The maximum reaction was calculated to be 244 kN or 55 kips. To demonstrate the flexibility of this structure compared to a cable-strut system, the spring was replaced with an infinitely stiff compression strut. With an elongated roof span of 29.7068 m and a service span of 29.6464 m the cables elongate 6.013 cm from their starting length of 29.7747 m. This equates to a strain of $\epsilon = 0.06013m/29.7747m = 0.0020195$. Using a Young's Modulus for steel of 29,000 ksi and four cables at the same sizes specified in Table 13, the steel cables produce a force of 843 kN or 190 kips at the supports. The use of the spring reduces support reactions by

71%. This demonstrates that the springs make a normal cable-strut system much more flexible. Truss, frame, arch, and beam systems would produce substantially higher loads as well. These however are not calculated in this work. Forces can be further reduced by decreasing the spring stiffness or increasing the depth to avoid having a shallow cable angle at the connection points.

The weight of the structure is also calculated below. Since the ETFE cushions and the cables were designed, exact values for their weight have been calculated. Table 14 summarizes the weights of the ETFE and cables for the entire roof panel highlighted in yellow in Figure 62.

Table 14: Summary of the Calculated Weights

System Component	Weight	Units	
Cables	47078	N	Calculated
ETFE	15150	N	Calculated
Total	62229	N	
Roof Section Area	1177	m^2	
Unit Weight	**52.9**	N/m^2	
Unit Weight	**1.10**	psf	

It is estimated that the roof weighs only 1.10 psf when including the cables and the triple layered ETFE cushions. This alone is a remarkable achievement. Including the approximations of the aluminum extrusions, springs, and air hoses creates Table 15.

Table 15: Approximation of Total Roof Weight

System Component	Weight	Units	
Cables	47078	N	
ETFE	15150	N	
Aluminum Extrusions	47078	N	Approximated
Springs	16020	N	Approximated
Air hoses	3139	N	Approximated
Total	128466	N	
Roof Section Area	1177	m^2	
Unit Weight	**109.1**	N/m^2	
Unit Weight	**2.28**	psf	

5.3 Experimental Model

An experimental modal was designed and built in order to demonstrate the flexibility of the system when compared to a cable-strut system. Figures 97 and 98 are two views of the model in design phase.

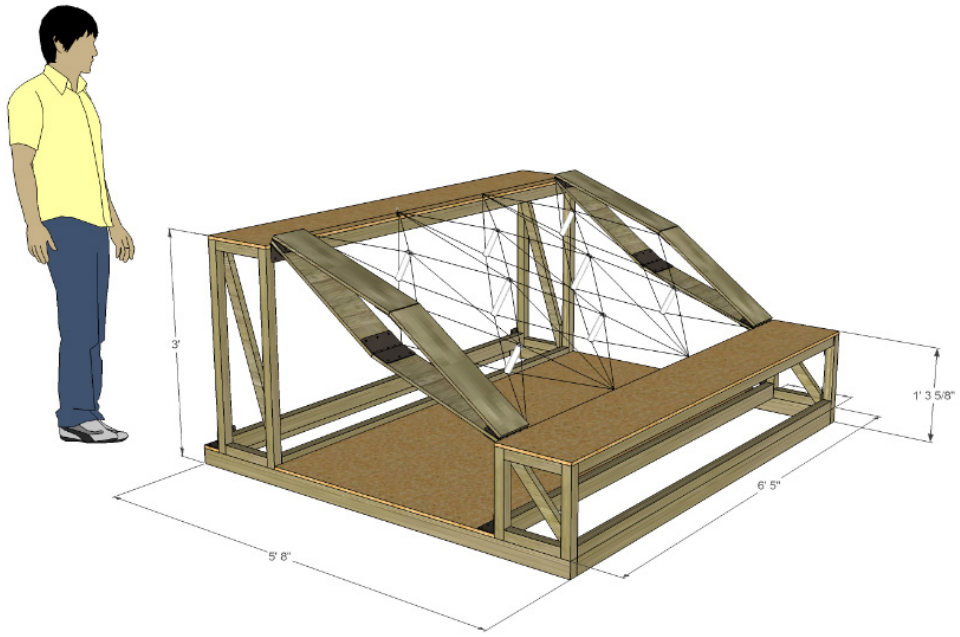

Figure 97: Isometric View of Model Design

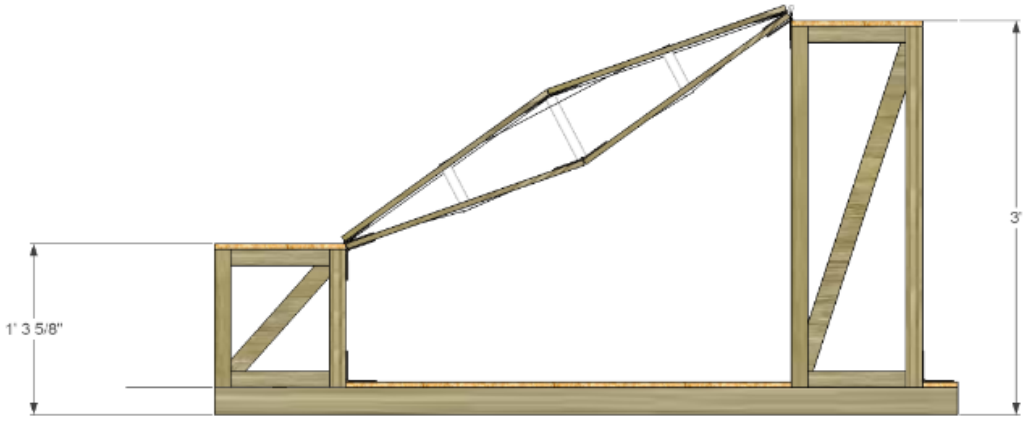

Figure 98: Side View of Model Schematic

Figures 99-103 show various views of the model in its completed form. Stainless steel wire rope was used in the weaving of the truss. Small compression springs were also ordered and fitted into two telescoping shafts to simulate the buckling restrained spring mechanism. The model roof spans between two supports that represent the neighboring buildings of the greenplex. The supports are mounted to the base on hinges so that the supports can pull or push apart from each other.

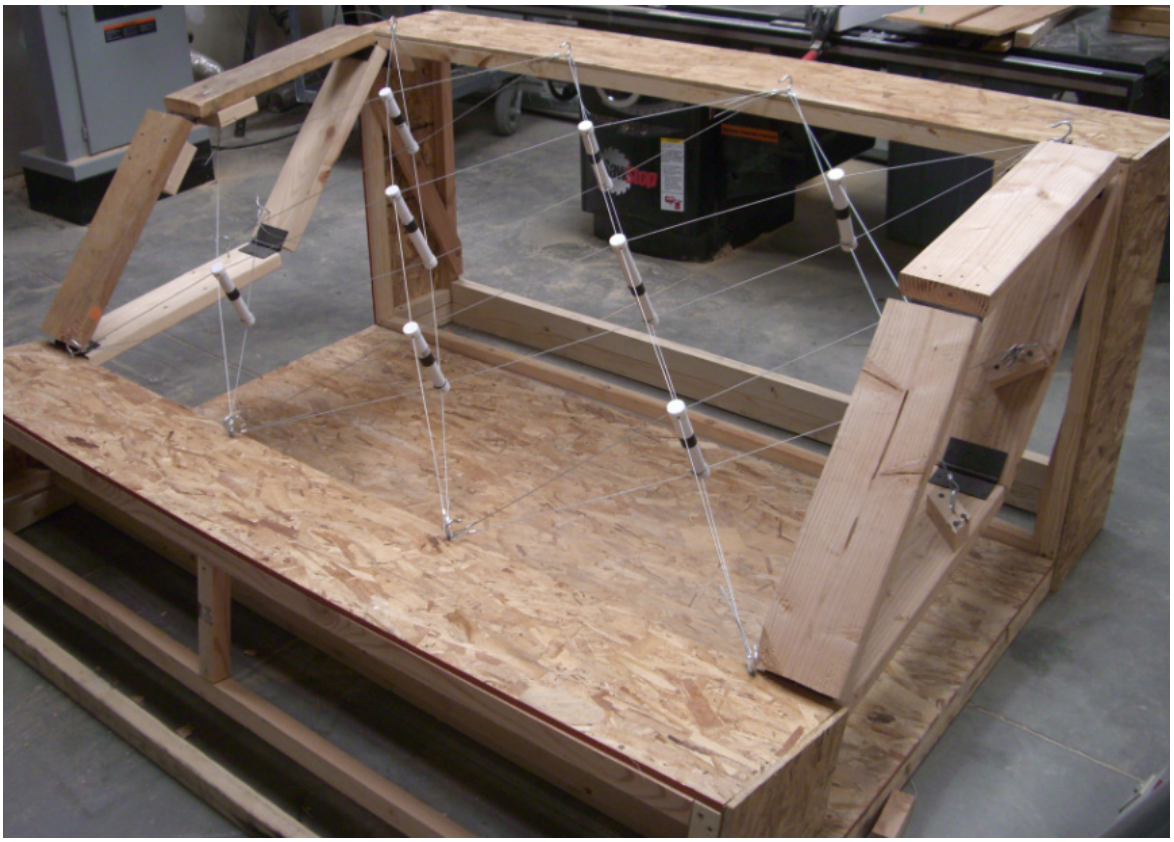

Figure 99: Isometric View of Actual Built Model

The coordinates of the tops and bottoms of the springs follow a parabolic shape while the cables in between them are essentially straight. This parabolic geometry was accomplished by ensuring that the springs all apply the same load into the cables in any deformed shape. Following Equation 5-16, springs were chosen to have the same material, coil diameter, and outer diameter. The only difference between springs was the two secondary springs were 3/4 the

length of the center springs. This gave the secondary springs the proper stiffness of 4/3 the center spring's stiffness.

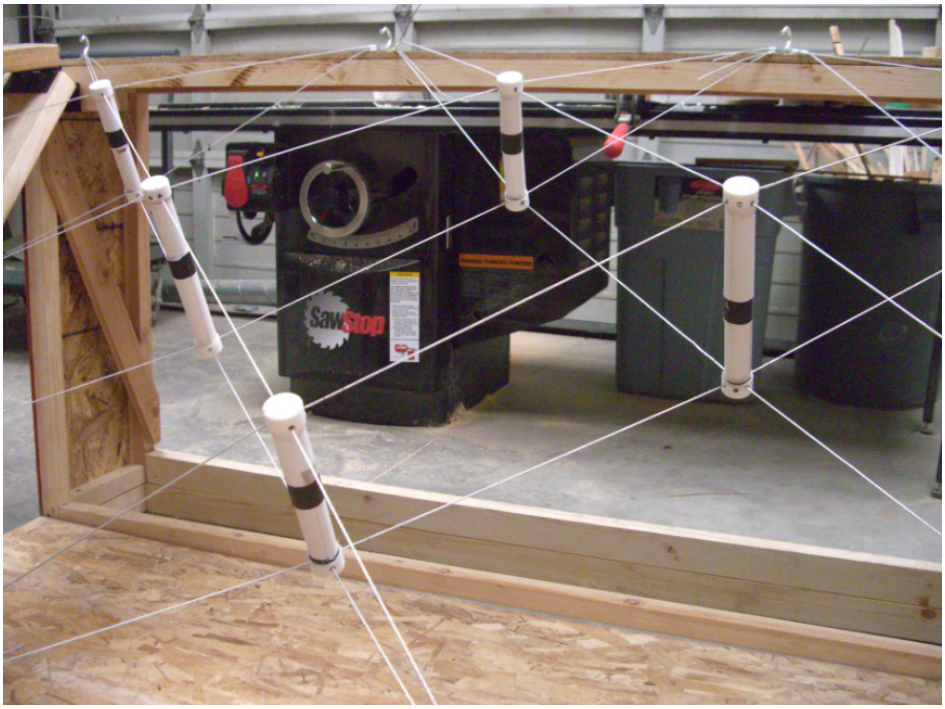

Figure 100: Close Up of Top and Bottom Cables

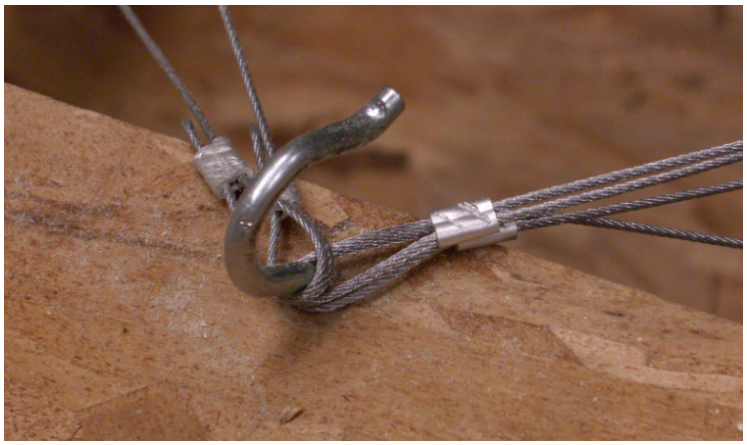

Figure 101: Close Up of Cable Attachments

Support reactions at the connections shown in Figure 101 are significantly less than if the springs were replaced with struts. This was easily demonstrated by inserting wooden dowels into the shafts instead of the springs as shown in Figure 102.

Figure 102: Dowels Used to Replace Springs

As a result the structure was so stiff that supports could hardly be separated. Even if the supports were designed to resist such loads the cables would likely undergo high material yielding. When the supports return back to their normal service span, with the permanently stretched cables in the roof, the entire structure would go slack and the strained cables would all need replacing. Using the highly elastic spring system proves effective in accepting support displacements without permanently damaging the structure.

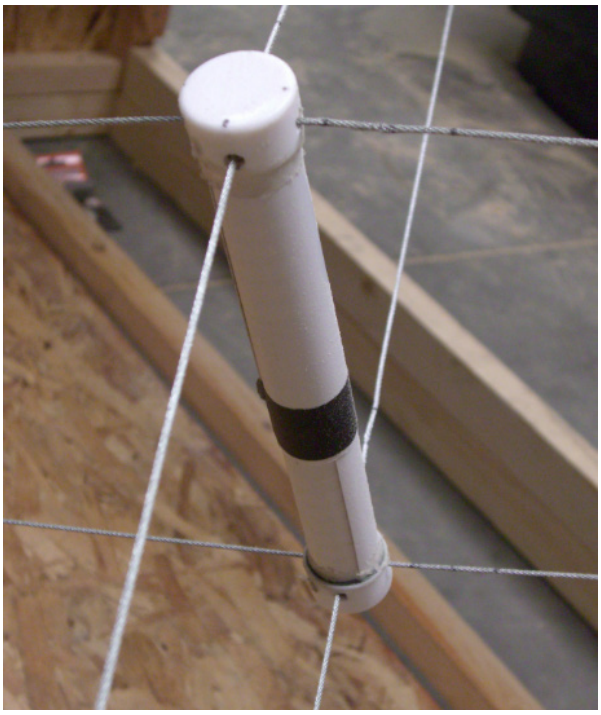

Figure 103: Close up of Spring

With the springs inserted into the shafts, instead of the wood dowels, the roof was easily expanded from its starting span of 44 inches to its maximum span of 46.5 inches. This equates to a strain of 5.68%. This displacement was easily achieved with hand pressure on the two sets of hinged beams shown in Figure 99. Further spans could also be achieved if even longer springs were used.

6 CONCLUSIONS

The first conclusion of this thesis is that the cable-spring support system proved effective in being light weight and exhibiting more flexibility than cable-strut systems. These were the primary goals of this research. These traits were quantified analytically in the example problem and verified in the experimental model.

The estimated roof weight, for the greenplex example problem, is about 2.28 psf. This is attributed to the light weight ETFE cushions and cables. The increased flexibility in the system compared to a cable-strut system was also calculated for the example problem. Using the same differential displacements, the support reaction produced by the cable-spring support system was calculated to be 71% less than a cable-strut system. The experimental model also demonstrates this correlation. The reduction in support reactions is expected to be even greater when compared to arches, frames, trusses, and beams.

The second conclusion of this thesis is that secondary goals of the conceptual and detailed design were completed for the greenplex design example. The conceptual design of the roof included: an on-demand air ventilation system; a specific cable-spring truss topology that prevents roof flutter; adequate roof slope to collect water at the building interfaces; and a repeatable cable topology that allows for the incremental construction of greenplex buildings overtime. The detailed design included the design of the ETFE cushions, springs, telescoping

tubes, and cables. During the detailed design, equations and graphs were developed for engineers to use when designing future cable-spring support systems.

Future research on this new structural system could include some of the following: wind load testing on scaled models; testing of seismic damping effects that the roof produces on the building systems that support it; and experimentation with other cable-spring support system topologies.

REFERENCES

Architen Landrell, (2012a). "ETFE: The New Fabric Roof." <http://www.architen.com/technical/articles/ETFE-the-new-fabric-roof> (2012)

Architen Landrell, (2012b). "ETFE Foil: A Guide to Design." <http://www.architen.com/.technical/articles/etfe-foil-a-guide-todesign> (2012)

ASCE, (2010a). "ASCE 19-10: Structural Applications of Steel Cables for Buildings." American Society of Civil Engineers, Reston, Virginia

ASCE, (2010b). "ASCE 55-10: Tensile Membrane Structures:" American Society of Civil Engineers, Reston, Virginia

ASCE, (2005). "ASCE 7-05: Minimum Design Loads for Buildings and Other Structures:" American Society of Civil Engineers, Reston, Virginia

Barnes, M., and Dickson, M. (2000). "Wide Span Roof Structures." Thomas Telford Publishing, London, England

Buitink Technology (2011). "Examples of detailing of ETFE." <http://www.buitink-technology.com/co.uk/page.asp?menu_id=864> (2012)

Cardoso, D., Michaud, D., Sass, L. (2011). "Soft Façade: Steps into the definition of a Responsive ETFE Façade for High-Rise Buildings." MIT

Cripps, A., Kolokotroni, M., Robinson-Gayle, S., and Tanno, S. (2001). "ETFE foil cushions in roofs and atria." Construction and Building Materials, 15. 323-327.

Galliot, C., Luchsinger, R.H. (2011). "Uniaxial and biaxial mechanical properties of ETFE foils." Swiss Federal Laboratories for Material Science and Technology, Duebendorf, Switzerland.

Hafner, A. and Moritz, K. (2010). "Transparency Carried by Air – Pneumatic ETFE-Foil-Cushion Technology." Structures Congress 2010, American Society of Civil Engineers Orlando, Florida.

Holmes, J. (2001). "Wind Loading on Structures." Chapter 10: Large roof and sports stadiums.

Jones, A., and Guthrie, A. (2003). "Creating the Garden of Eden- Engineering the Worlds Largest Greenhouse." The Royal Academy of Engineering, London.

Kloiber, L., Eckmann, D., Meyer, T., and Hautzinger, S. (2004). "Design Considerations in Cable-Stayed Roof Structures." The North American Steel Construction Conference, Modern Steel Construction.

Koch, K.M. (2004). “Membrane Structures.” Prestel Verlag, Munich, Germany

LeCuyer, A. (2008). “ETFE: Technology and Design.” Birkhauser Verlag AG, Basel, Germany

Minger, W., Yuanyuan W., and Jae-Yeol, K. (2011). “ETFE Foil Spring Cushion Structure and its Analytical Method.” Thin Walled Structures 49, 1184-1190

Moritz, K., (2007). “Bauweisen der ETFE-Foliensysteme.” Stalbau 76 (5), 336-342.

Moritz, K., and Hafner, A. (2010). “Transparency Carried By Air – Pneumatic ETFE-Foil-Cushion Technology”, Structures Congress, American Society of Civil Engineers (ASCE)

Polymers: A Property Database, (2012). <http://www.polymersdatabase.com> (2012)

Reid, R.L. (2009). “150 m Tall ‘Tent’ Designed as Kazakh Entertainment Center.” <http://civil-engineering.asce.org/wps/portal/ce/c0/04_SB8K8xLLM9MSSzPy8xBz9CP0os3iLkCAPEzcPIwP_ACc3AyMXF4sQk6AQY_cAE_1I_ShznPIhhvohIBMz9SNNTAxNQMxi_UgDEF2gH2loARbILy1KTtWPLE5NLErO0C_ITkyqSk2qcnRUVAQAclu6tg!!/> (2012)

Robinson, L.A. (2005). “Structural Opportunities of ETFE (ethylene tetrafluoroethylene).” M.S. thesis, Massachusetts Institute of Technology, Cambridge, MA

SCNZ, (2011). “Forsyth Barr Stadium by the Fabricators.” <http://www.scnz.org/magazine/2011/10/forsyth-barr-stadium-by-the-fabricators/> (2012)

SolarNext, (2012) <http://www.solarnext.eu/ger/home/home_ger.shtml> (2012)

Tanno, S. (1997). “ETFE Cushions as an Alternative to Glass for Atriums and Rooflights.” The International Conference on Building Envelope Systems and Technologies ’97, Bath, UK, Centre for Window and Cladding Technology.

Topping, B.H.V., and P. Iványi (2007). “Computer Aided Design of Cable Membrane Structures.” Saxe-Coburg Publications, Kippen, Stirlingshire, Scotland

Vector Foiltec, (2012a). <http://www.vector-foiltec.com/en/profile/history.html> (2012)

Vector Foiltec, (2012b). <http://www.vector-foiltec.com/en/technical/structural.html>(2012)

Vector Foiltec, (2012c). <http://www.vector-foiltec.com/en/technical/fire.html>(2012)

Vector Foiltec, (2012d). <http://www.vector-foiltec.com/en/technical/durability.html> (2012)

Vector Foiltec, (2012e). <http://www.vector-foiltec.com/en/technical/variable-skins.html> (2012)

Vector Foiltec, (2012f). <http://www.vector-foiltec.com/en/projects/pages/gb-london-kingsdale-school.html> (2012)

Vector Foiltec, (2012g). <http://www.vector-foiltec.com/en/projects/pages/gb-cornwalleden.html> (2012)

Vector Foiltec, (2012h). <http://www.vector-foiltec.com/en/projects/pages/khan-shatyr-entertainment-center-astana.html> (2012)

Vector Foiltec, (2012i). <http://www.vector-foiltec.com/en/projects/pages/cn-peking-green-plaza.html> (2012)

Vector Foiltec, (2012j). <http://www.vector-foiltec.com/en/projects/pages/forsyth-barr-stadium-dunedin-otago.html> (2012)

Winser, R., Thompson, P. (2002). "ETFE Foil Cushions as an Alternative to Glass for Roofs and Atria." Department of the Environment, Transport and the Regions, Documents 1-3

Winser, R., Thompson, P. (2003). "ETFE Foil Cushions as an Alternative to Glass for Roofs and Atria." Department of the Environment, Transport and the Regions, Document 4

Visit all the World, (2012) <http://www.visitalltheworld.com/blog/archives/tag/allianz-arena> (2012)

Winkler, J. (2009). "Kriechverhalten von ETFE-Folien im konstruktiven Ingenieurbau" M.S. thesis, Technische Universität Berlin, Berlin, Germany.